THE ROLE OF PROTEIN SUBUNITS IN SUPEROXIDE GENERATION BY THE CYTOCHROME bc_1 COMPLEX FROM *RHODOBACTER SPHAEROIDES*

By

YING YIN

Bachelor of Science

Sichuan University

Chengdu, Sichuan, China

2003

Submitted to the Faculty of the
Graduate College of the
Oklahoma State University
in partial fulfillment of
the requirements for
the Degree of
DOCTOR OF PHILOSOPHY
December, 2009

THE ROLE OF PROTEIN SUBUNITS IN

SUPEROXIDE GENERATION BY

THE CYTOCHROME bc_1 COMPLEX FROM

RHODOBACTER SPHAEROIDES

Thesis Approved:

Dr. Chang-An Yu

Thesis Adviser

Dr. Linda Yu

Dr. Robert Burnap

Dr. Robert Matts

Dr. Andrew Mort

Dr. A. Gordon Emslie

Dean of the Graduate College

ACKNOWLEDGMENTS

I would like to express my sincere appreciation to my advisors Dr. Chang-An Yu and Dr. Linda Yu for their intelligent supervision, encouragement, guidance, support, and inspiration during my PhD study. My sincere appreciation extends to my other committee members Dr. Robert Matts, Dr. Andrew Mort, and Dr. Robert Burnap, whose guidance, assistance, encouragement were also invaluable.

I would like to thank former and current students and post doctorates in Dr. Yu's lab for their assistance and friendship.

Finally, I would like to give my great appreciation to my parents for their wonderful love, understanding, and encouragement.

TABLE OF CONTENTS

LIST OF TABLES

LIST OF FIGURES

NOMENCLATURE

ADP	Adenosine diphosphate
ATP	Adenosine triphosphate
AA	Antimycin A
BSA	Bovine serum albumin
CMC	Critical micellar concentration
Cyt.	Cytochrome
DM	Dodecylmaltoside
DMSO	Dimethyl sulfoxide
DOC	Deoxycholate
DSC	Differential scanning calorimeter
EDTA	Ethylenediaminetetraacetic acid
EPR	Electron Paramagnetic Resonance
FPLC	Fast protein liquid chromatography
GST	Glutathione-S-transferase
ICM	Intracytoplasmic membrane
IM	Inner membrane
IMS	Inter-membrane space
ISC	Iron-sulfur cluster
ISP	Rieske iron-sulfur protein

IPTG	Isopropyl β-D-thiogalactopyranoside
kDa	Kilodaltons
kb	Kilo base pair
LB	Lennox L. Broth
LM	Dodecylmaltoside
MCLA	6-(4-methoxyphenyl)-2-methyl-3,7-dihydroimidazol [1,2-α]pyrazin-3-one hydrochloride
MOAS	β-methoxyacrylate stilbene
NADH	Nicotinamide adenine dinucleotide (reduced form)
NQNO	2-*n*-nonyl-4-hydroxyquinoline *N*-oxide
$O_2^{\cdot -}$	Superoxide anion radical
OG	N-octyl-D-gluocopyranoside
Pi	Inorganic phosphate
Psi	Pound per square inch
PAGE	Polyacrylamide gel electrophoresis
PBS	Phosphate buffered saline
PCR	Polymerase chain reaction
PL	Phospholipid
PMSF	Phenylmethylsulfonyl fluoride
$Q^{\cdot -}$	Ubisemiquinone
Q	Ubiquinone
QH_2	Ubiquinol
Q_2H_2	2,3-dimethoxy-5-methyl-6-geranyl-1,4- benzoquinol

$Q_0C_{10}BrH_2$	2,3-dimethoxy-5-methyl-(10-bromodecyl)1,4-benzoquinol
R. sphaeroides	*Rhodobacter sphaeroides*
ROS	Reactive oxygen species
SC	Sodium cholate
SDS	Sodium dodecylsulfate
SOD	Superoxide dismutase
STIG.	Stigmatellin
TM	Transmembrane
UHDBT	5-undecyl-6-hydroxy-4,7-dioxobenzothiazole
XO	Xanthine Oxidase
β-ME	β-mercaptoethanol
ε	Extinction coefficient
[2Fe-2S]	Rieske iron-sulfur cluster

CHAPTER I

INTRODUCTION

Mitochondrial Electron Transport Chain

All living cells need energy to support themselves. More than 90% of the energy required for an aerobic cell is provided through a process called oxidative phosphoration, which occurs in the mitochondria. Oxidative phosphoration is carried out in the inner mitochondrial membrane by the electron transport chain and ATP synthase (1, 2).

The mitochondrial electron transport chain is composed of four enzyme complexes: NADH : ubiquinone oxidoreductase (complex I); succinate : ubiquinone oxidoreductase (complex II); cytochrome bc_1 complex (ubiqinol : cytochrome *c* oxidoreductase, or complex III); and cytochrome *c* oxidase (complex IV). The electron transport chain starts with NADH and succinate, which are electron donors to complex I and complex II, respectively. Complexes I and II function as dehydrogenases that transfer electrons from NADH (-300 mV), and succinate (30 mV) to ubiquinone (45 mV). Subsequently, the bc_1 complex transfers electrons from ubiquinol to cytochrome *c*, which in turn reduces oxygen in a reaction catalyzed by complex IV (cytochrome *c* oxidase). The overall scheme of the mitochondrial electron transfer pathway is shown on the next page in Figure 1.

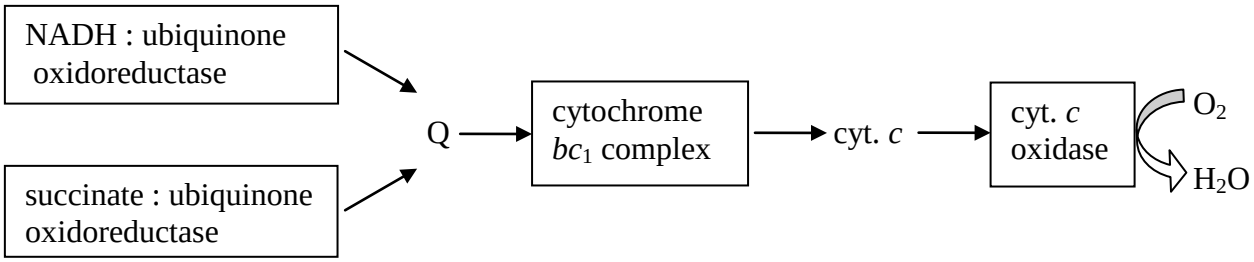

Figure 1. **The scheme of the electron transfer pathway in mitochondria.**

The electron transfer is coupled to the proton translocation from the matrix to the intermembrane space, which generates a proton gradient and membrane potential. This coupling occurs in all of the electron transfer complexes except complex II , as shown in Figure 2 on the following page. The generated proton motive force is utilized for the synthesis of ATP by the ATP synthase complex (3). The ATP synthase is comprised of two functional subunits, F_0 within the inner membrane and F_1 within the matrix. F_1 is the water-soluble catalytic subunit which binds ADP and Pi to generate ATP. The F_0 subunit is a hydrophobic protein that contains a proton translocating channel. The proton motive force drives the proton though the membrane via F_0. The ring of c-subunit in the F_0 subunit rotates as the protons pass through the membrane. The c-ring is tightly attached to the asymmetric central stalk which rotates within the $\alpha_3\beta_3$ of F_1 causing the 3 catalytic nucleotide binding sites to go through a series of conformational changes that lead to ATP synthesis.

The Cytochrome bc_1 Complex

The cytochrome bc_1 complex and the electron transport chain – The cytochrome bc_1 complex (complex III, or ubiquinol-cytochrome *c* reductase) is a central component of electron transport chains of mitochondria and many respiratory and photosynthetic prokaryotes. It is an analogous complex to cytochrome b_6f in the photosynthetic chain of oxygenic photosynthesis (4). The bc_1 complex catalyzes the two-electron oxidation of ubiquinol with the one electron reduction of cytochrome *c*, which meanwhile deposits four protons to the positive side of the membrane, resulting in the generation of a membrane potential and proton gradient. The following equation describes the overall

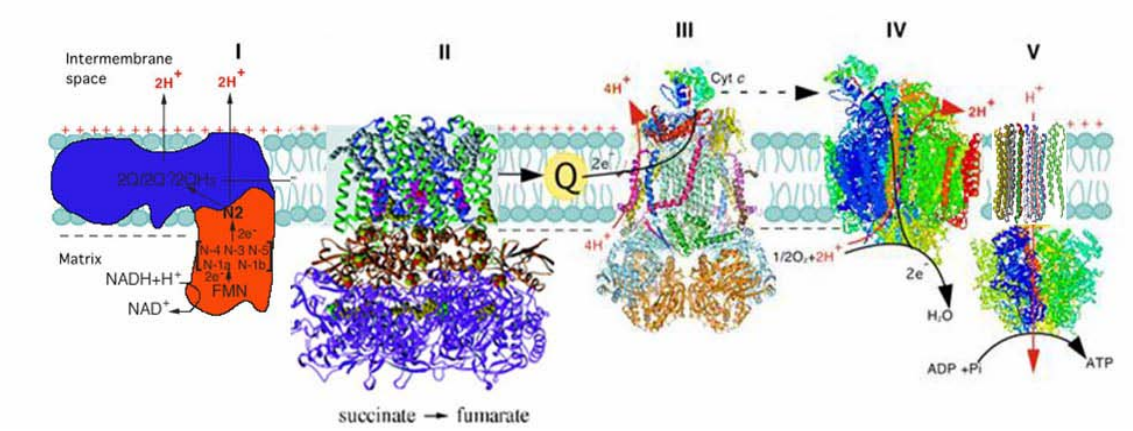

Figure 2. **Mitochondrial electron transport chain**

reaction catalyzed by the cytochrome bc_1 complex.

$$QH_2 + 2H^+_n + 2 \text{ cytochrome } c^{3+} \longrightarrow Q + 4H^+_p + 2 \text{ cytochrome } c^{2+}$$

The "p" and the "n" in the above equation refer to the positive side and negative side of the membrane, respectively.

The cytochrome bc_1 complexes from all species contain three core subunits: cytochrome *b*, cytochrome c_1, and Rieske Iron-Sulfur protein (ISP) which house four redox centers: two *b* type cytochromes, b_L (b_{566}) and b_H (b_{562}), one *c* type cytochrome (c_1), and a high potential Rieske [2Fe-2S] cluster, respectively. In addition to these three core subunits, varying numbers of non-redox group containing subunits called supernumerary subunits are present in the cytochrome bc_1 complexes from different species (Table 1, next page). Although the role of supernumerary subunits has not been fully understood, it is generally believed that the main functions of these supernumerary subunits are to maintain the structural integrity of the bc_1 complexes (5, 6).

In addition to the respiratory system, the bc_1 complex is also found in bacterial photosynthetic electron transport systems. It acts as a central component of a cyclic photosynthetic pathway in the photosynthetic purple non-sulfur bacterium *Rhodobacter sphaeroides*, as shown in Figure 3, pathway A on page 7. After becoming excited by light energy, the P_{870} (two bacteriochlorophyll molecules) inside the reaction center becomes a strong reducing agent. And then it gives the electron to a bacteriopheophytin *b* molecule (BPh), a bound quinone at the Q_A site, and eventually to a bound quinone at the Q_B site. Upon accepting the two electrons, the quinone at the Q_B site becomes fully reduced Q^{2-}, and immediately takes up two protons from the cytoplasm to form QH_2. The QH_2 is then released and acts as the electron donor for the cytochrome bc_1 complex,

Table 1. **The number of subunits in bc_1 complexes from different species**

Species	Core subunit	Supernumerary subunit
Bovine heart	3	8
Potato	3	7
Chicken heart	3	7
Yeast	3	7
Rhodobacter sphaeroides	3	1
Rhodobacter capsulatus	3	0
Human	3	8

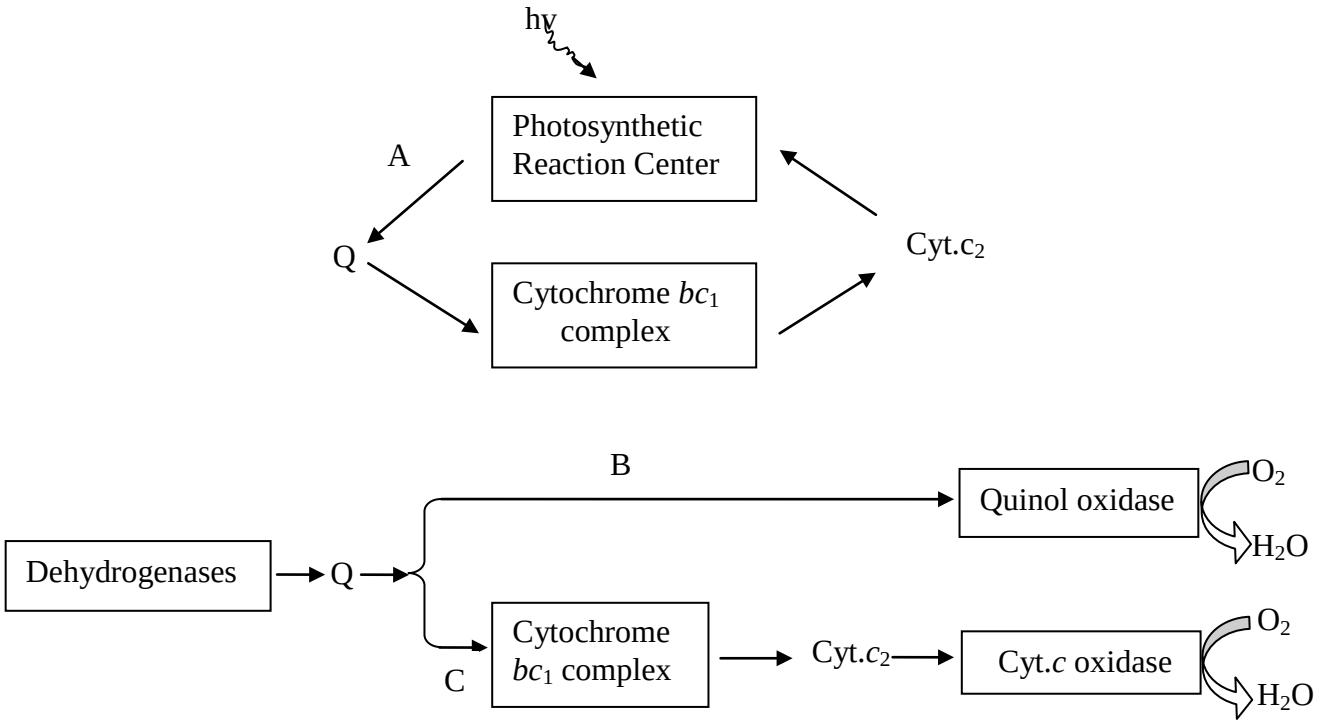

Figure 3. **Electron transfer pathways in R. *sphaeroides*.** Pathway A: Anaerobic, photosynthetic cycle; Pathway B, C: Aerobic growth in the dark.

which in turn transfers the electron to cytochrome c_2. As in the mitochondrial cytochrome bc_1 complex, four protons are translocated across the membrane for every two electrons transferred through this photosynthetic bacterial bc_1 complex. The reduced cytochrome c_2 then carries electrons back to the photosynthetic reaction center and as a result, it reduces the P_{870}. Therefore, in this photosynthetic cyclic electron transfer pathway, there is no need for an exogenous electron donor or final electron acceptor. Electrons are kept cycling in this pathway with the supply of light energy to produce a proton motive force from the bc_1 complex for ATP synthesis. The cytochrome bc_1 complex is not an absolutely essential respiratory component during aerobic dark growth of this photosynthetic bacteria. It is, however, absolutely essential for anaerobic, photosynthetic growth of this bacteria (Figure 3, above).

The Q-Cycle Mechanism – Based on the redox potential of the four prosthetic groups of the bc_1 complex, the electron transfer through the cytochrome bc_1 complex is shown in the scheme below:

$$QH_2 \longrightarrow b_L \longrightarrow b_H \longrightarrow ISP \longrightarrow \text{cyt. } c_1 \longrightarrow \text{cyt. } c$$

However, this scheme cannot explain the 2 H^+ / 1 e^- stoichiometry observed during the cytochrome bc_1 complex catalysis (7), as it can only show a 1 H^+/e^- stoichiometry. Furthermore, it fails to explain the observed phenomenon of "oxidant-induced reduction of cytochrome *b*" (8). In the presence of antimycin, the addition of a pulse of oxygen to slowly respiring mitochondria causes a transient increased reduction of cytochrome b_L with a rate comparable to that of the oxidation of cytochrome c_1. In 1976, Peter Mitchell proposed the "protonmotive Q-cycle mechanism" (Figure 4A, below) for the electron and proton transfer mechanisms in the cytochrome bc_1 complex (9). This mechanism

A.

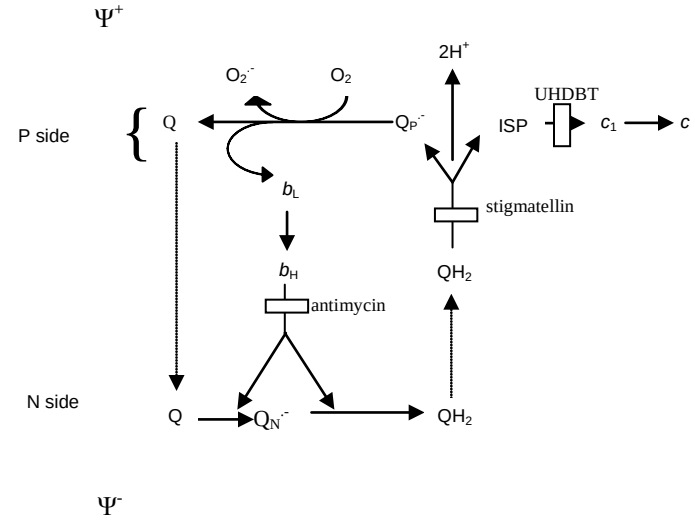

B.

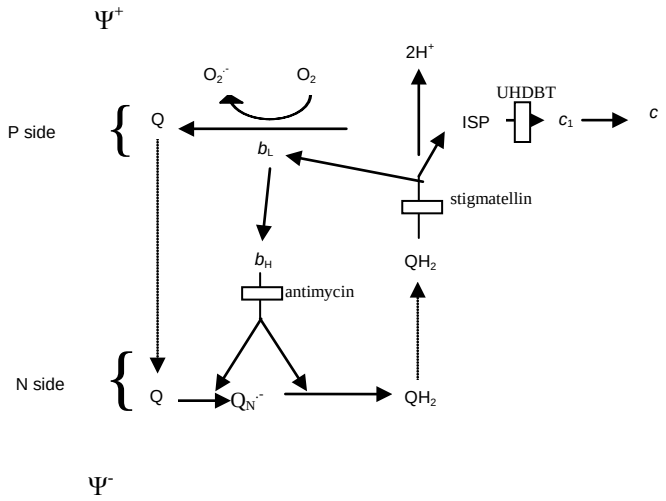

Figure 4. **The protonmotive Q-cycle mechanism.** (A) Sequential bifurcated oxidation of ubiquinol at the Q_P site. (B) Concerted bifurcated oxidation of ubiquinol at the Q_P site.

accommodates the observed 2 H^+ / 1 e^- stoichiometry and oxidant-induced cytochrome *b* reduction. There are two key features of this mechanism: 1) the presence of physically separated quinol oxidation (Q_P) and quinone reduction (Q_N) sites, and 2) the bifurcation of electron transfer from the ubiquinol at the Q_P site.

It has been proposed by Mitchell (9) that the first electron from ubiquinol at the Q_P site is transferred to a high-potential chain consisting of the Rieske iron-sulfur cluster and the heme c_1, and then cytochrome *c*. The second electron from formed $Q^{\cdot-}$ is passed to a low-potential chain containing heme b_L and heme b_H, and then to a ubiquinone at the Q_N site to form a stable ubisemiquinone ($Q^{\cdot-}$). This completes half of the Q-cycle, then a second ubiquinol is bifurcated and oxidized at the Q_P site, and the electron from heme b_H now reduces the ubisemiquinone formed at the Q_N site during the first cycle. Subsequently, two protons are taken up from the N-side to form QH_2 thereby completing the Q-cycle. In this proposed Q-cycle mechanism, bifurcated oxidation of ubiquinol at the Q_P site proceeds by sequentially giving two electrons to ISC and heme b_L (the sequential mechanism). However, the inability to detect a functional $Q^{\cdot-}$ at the Q_P site and the observation that the rate of b_L reduction is the same as ISP reduction (10) encouraged investigators in the field, including our group, to propose that bifurcated oxidation of ubiquinol at the Q_P site proceeds by simultaneously giving the two electrons to ISC and heme b_L (the concerted mechanism, Figure 4B, page 9). The concerted mechanism excludes the formation of the semiquinone radical at the Q_P site. The overall Q-cycle reaction is represented by the following equation:

$$QH_2 + 2 \text{ cyt } c^{3+} + 2H^+_N \longrightarrow Q + 2 \text{ cyt } c^{2+} + 4H^+_P$$

Three-dimensional crystal structure of mitochondrial cytochrome bc_1 complex –

Overall structure of the bovine mitochondrial bc_1 complex – The first Cytochrome bc_1 complex crystal structure with a 2.9 Å resolution from bovine heart was determined by our group in 1997 in collaboration with Dr. Deisenhofer's lab (16, Figure 5, next page). Since then, mitochondrial bc_1 complexes from chicken (17) and yeast (18, 19) have become available with X-ray diffraction at about 3 Å. In our $I4_122$ structure, the bc_1 complex contains 4,330 amino acid residues with a total molecular weight of 496 kDa. The complex exists as a pear-shaped, intertwined dimer with a diameter of 130 Å at its widest point in the matrix and is 155 Å in height. The height of 155 Å can be divided into three regions: inter-membrane space region (38 Å), transmembrane region (42 Å), and matrix region (75 Å). Each monomer contains three catalytic subunits and eight supernumerary subunits. The majority of the bc_1 complex is located in the matrix. This region contains subunits I, II, VI, and IX, the N-terminal part of subunit VII, and the C-terminal part of ISP. The transmembrane region consists of thirteen transmembrane helices in each monomer—eight from cytochrome *b* plus one each from cytchrome c_1, ISP, and subunits VII, X, and XI. The inter-membrane space region houses the functional domains of cytchrome c_1 and ISP, as well as subunit VIII (20).

The structure of cytochrome b (Figure 6, page 13) – Cytochrome *b*, the only mitochondrially encoded protein in the bc_1 complex, is one of the three catalytic subunits of this complex. Both the N-terminal and C-terminal of this subunit are located in the mitochondrial matrix. There are two *b*-type hemes within the cytochrome *b* subunit: the high-potential heme b_H, which is close to the matrix side of cytochrome *b*, and the low-potential heme b_L located close to the intermembrane space side of the subunit.

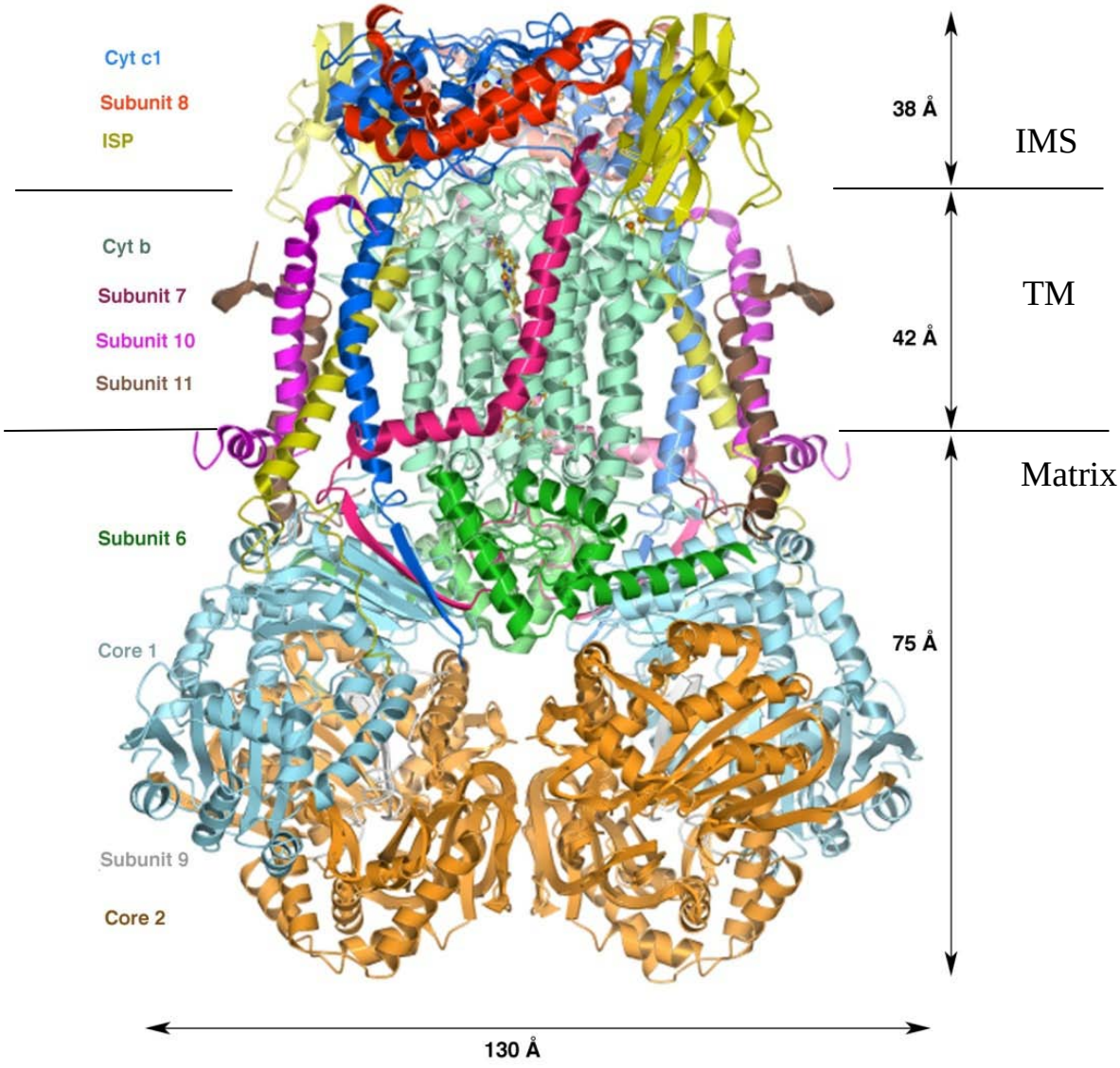

Figure 5. **The structure of the dimeric bovine mitochondrial cytochrome bc_1 complex shown in ribbon form (21).** The two parallel lines delineate the boundary of the mitochondrial inner membrane. The mitochondrial inter-membrane space (IMS), the transmembrane region (TM), and the mitochondrial matrix (Matrix) are as labeled.

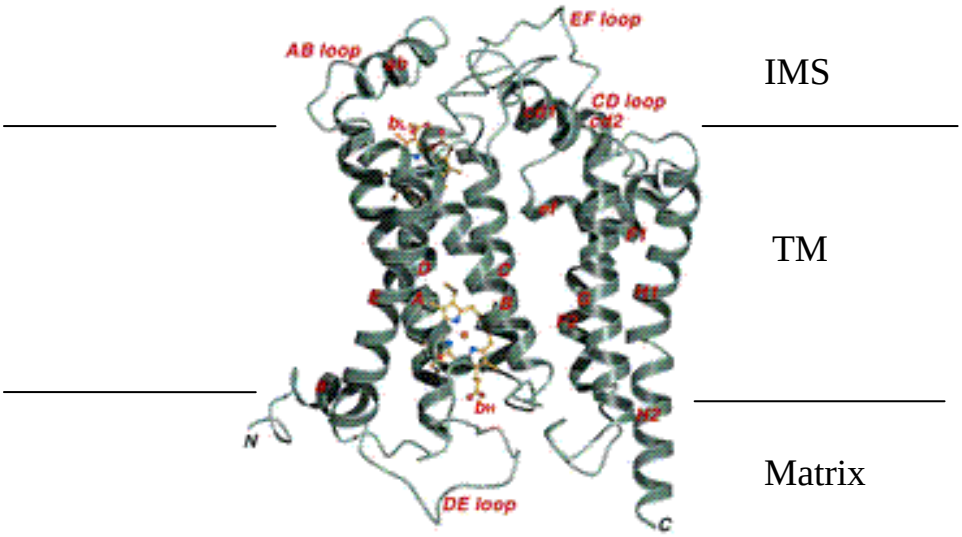

Figure 6. **Ribbon structure of the mitochondrial cyt. *b* subunit (21).** The ribbon representation of cyt. *b* shows eight TM helices (as labeled). Four prominent extra-membrane loops including AB, CD, DE, and EF are also labeled. The b_L and b_H hemes are shown as stick models with the carbon atoms in yellow, nitrogen in blue, and oxygen in red. The mitochondrial inter-membrane space (IMS), the transmembrane region (TM), and the mitochondrial matrix are as labeled.

Cytochrome *b* is the Q-binding subunit. It contains two Q binding sites: the Q_P pocket and the Q_N pocket. They are in close vicinity to hemes b_L and b_H, respectively. Cytochrome *b* has eight transmembrane helices named A to H. These eight helices form two bundles: helices A-E are in the first bundle, and F-G are in the second bundle. The two bundles are in close contact on the matrix side and are separated on the intermembrane space side, creating a gap between them to form the Q_P pocket (16). The two b-type hemes are bound within the first bundle between the transmembrane helices B and D. His-83 and His-182 are the ligands for heme b_L while heme b_H is ligated by His-97 and His-196. Four long loops (AB, CD, DE, and EF) and three short loops (BC, FG, and GH) connect these eight transmembrane helices. The DE loop is on the matrix side, and the other three long loops are on the intermembrane space side of the membrane (16). The CD loop has two short helices, named cd1 and cd2, which are close to the Q_P pocket, and form one part of the docking site for ISP. The EF loop bridges between the two helical bundles and forms another part of the ISP interaction site. The iron-iron distance between heme b_L and b_H is 21 Å, which is in good agreement with the predicted distance of 22 Å from previous studies (23). The distance between the two b_L hemes in the two monomers is 21 Å, which is short enough to allow electron transfer between them (24).

The structure of cytochrome c_1 (20) (Figure 7, below) – Cytochrome c_1 contains seven helical structures, including the C-terminal transmembrane helix. They are α1, α1', α1'', and α2 to α6. There is one distorted double-stranded β-sheet (β-1 and β-2) between helices α3 and α5. The subunit houses one redox prosthetic group heme c_1. It is ligated with residues His-41 and Met-160, and is covalently anchored to Cys-37 and Cys-40. In this subunit, there are three docking sites for cytochrome *c*, ISP, and subunit 8

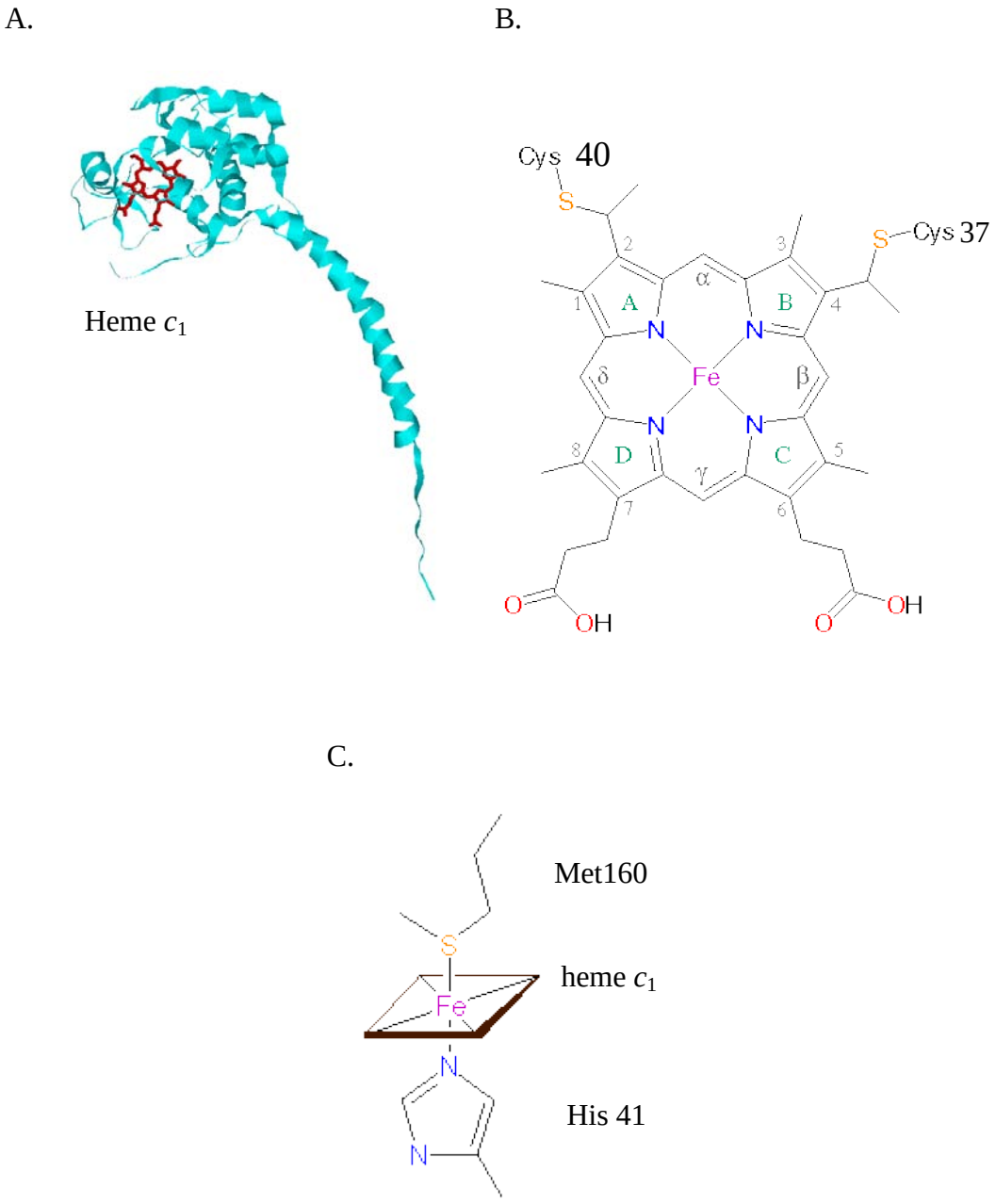

Figure 7. **Structure of cytochrome c_1.** (A) The overall structure of cytchrome c_1, heme c_1, is shown as a stick mode in red; (B) the structure of heme c_1; (C) the ligands for heme c_1.

(hinge protein), respectively. The N- terminal extension before helix α1, together with loop α3-β1, forms a docking surface for subunit 8. Helix α1' and loop α3-β1 contain 10 acidic amino acids, many of which point to the intermembrane space side and surround the heme c_1 crevice, which is the most likely binding site for cytochrome *c*. Loop α1''-α2, together with β2, form a docking site for ISP in the $P6_522$ form (20).

The structure of ISP (25, Figure 8, below) – ISP contains three domains: the membrane-spanning N-terminal domain (tail) consisting of residues 1-62; the extrinsic C-terminal domain (head), which is a rigid, compact, and flat-spherical-shaped structure, containing residues 73-196; and the flexible domain (neck), which links the head and tail domain, containing residues 63-72. The head domain contains three layers of anti-parallel β-sheets composed of ten β-strands (β1-β10). The only α helix and loop are located between β3 and β4. The iron-sulfur cluster is located at the tip of the head domain. The [2Fe-2S] cluster is ligated by two cysteine and two histidine residues: Cys-139 and His-141 in the loop β4-β5, and Cys-158 and His-161 in the loop β6-β7. The two highly conserved cysteine residues Cys-144 in the loop β4-β5 and Cys-160 in the loop β6- β7 form a disulfide bond to stabilize the fold around the cluster. The cluster is also stabilized by multiple hydrogen bonds. Compared to other iron-sulfur clusters, this [2Fe-2S] cluster has much higher redox potential. Multiple factors cause this high potential: 1) the overall charge of the cluster, 0/-1 for the oxidized and reduced state, respectively, compared to -2/-3 for [2Fe-2S] clusters with four- cysteine coordination; 2) the electronegativity of the histidine ligands; 3) the presence of multiple hydrogen bonds to the bridging and terminal sulfur atoms; and 4) the solvent exposure of the Fe(II) (25).

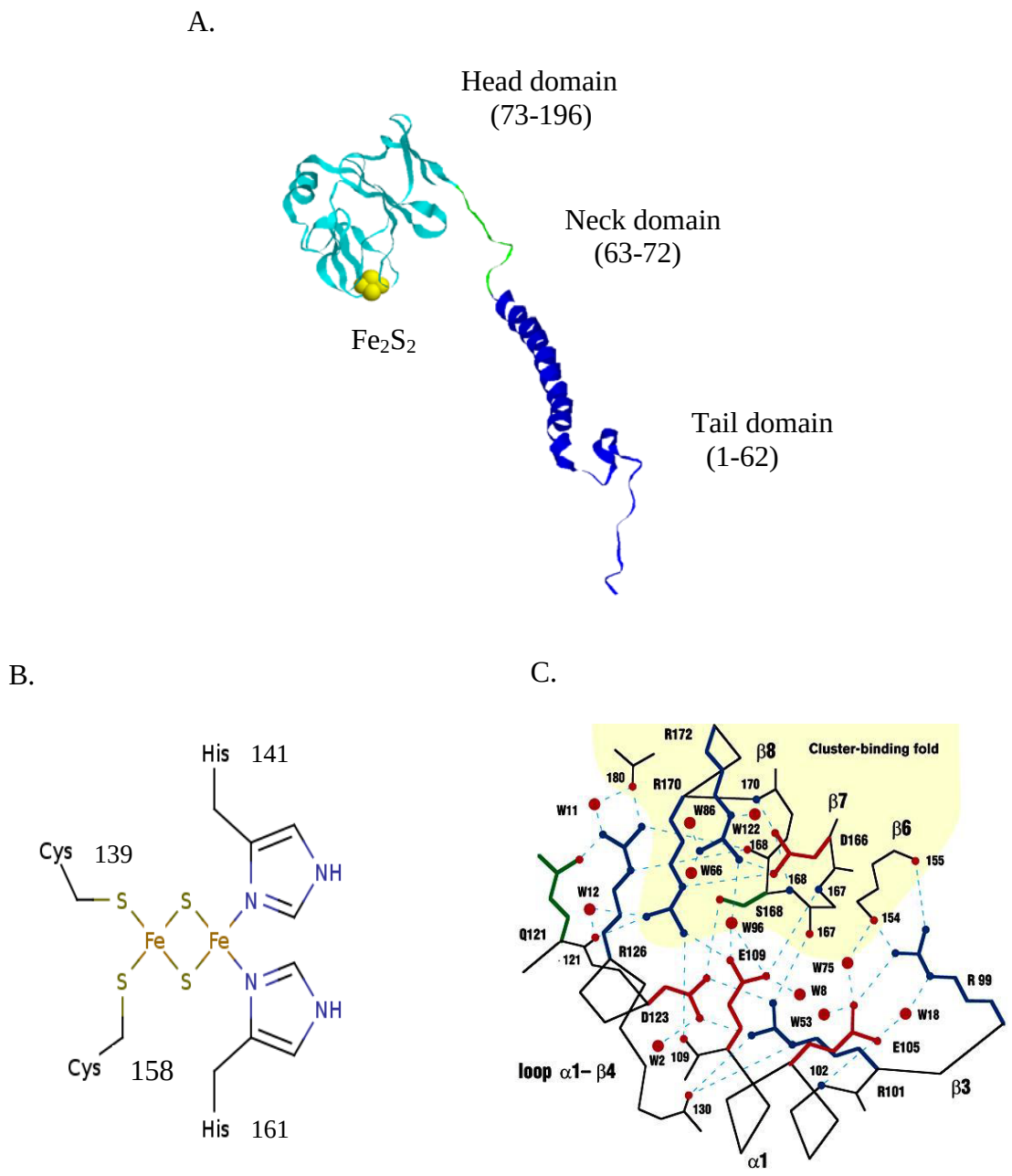

Figure 8. **Structure of the Rieske Iron-sulfur Protein (ISP).** (A) The overall structure of ISP; the [2Fe-2S] cluster is shown with spacefill in yellow. The head domain is in cyan, the neck domain is in green, and the tail domain is in blue. (B) The ligands for the [2Fe-2S] cluster. (C) The salt bridge/hydrogen bond network around the [2Fe-2S] cluster.

The cytochrome bc_1 complex functioning as a dimer – The structural information of the bc_1 complex (16) not only reveals the location of prosthetic groups and inhibitor binding sites, but also suggests both that the complex exists as a functional dimer and that there is the possibility for domain movement of the ISP head during bc_1 catalysis.

The suggestion of the complex functioning as a dimer stems from the following structural data (16-19): (i) The two ISP subunits in the two bc_1 monomers are in an intertwined arrangement such that the head domain of ISP in one monomer is physically close to and interacts with the cytochrome *b* and cytochrome c_1 in the 2-fold symmetry-related other monomer; (ii) The distance between the two Fe atoms of the two b_L hemes in the two monomers is only 21 Å, which is approximately the same as that between heme b_L and b_H within one monomer. This distance is short enough to allow electron transfer between the two b_L hemes; (iii) The presence of two apparently non-communicating internal cavities in the dimeric complex, each connecting the Q_P pocket of one monomer to the Q_N pocket of the other monomer.

Recently the existence of an intertwined dimer in solution was confirmed in *R. sphaeroides* bc_1 complex (26) with the formation of a four subunit (two ISPs and two cytochrome *b*s) adduct by two inter-subunit disulfide bonds between two engineered cysteine pairs: one at cyt. *b* and the head domain of ISP, and the other at cytochrome *b* and the tail domain of ISP.

The movement of the ISP head domain during bc_1 catalysis – The X-ray structure of the beef mitochondrial bc_1 complex (16) suggests the movement of the ISP head domain during bc_1 catalysis. This suggestion stems from the following observations (i) the anomalous scattering signal of the [2Fe-2S] cluster is much weaker than that in the

heme iron of b_L and b_H; (ii) The distance between the iron-sulfur cluster and cytochrome c_1 is 31 Å, which is too large to account for the observed high electron transfer rate between these two prosthetic groups; and (iii) The head domain of ISP is at different positions in the presence of different inhibitors.

This movement hypothesis is further supported by genetic studies of the ISP neck region in *Rhodobacter sphaeroides, Rhodobacter capsulatus,* and yeast bc_1 complexes (27-32), and of fixing the head domain of ISP at the "*b*" or "c_1" position through a inter-subunit disulfide bond formed between the ISP head and cytochrome *b* or the ISP head and cytochrome c_1 from *R. sphaeroides* (33, 34). The increase in the neck rigidity through proline substitution, deletion, or insertion of amino acid residues and the decrease in bc_1 activity indicate that the head domain movement of ISP requires the flexibility of the ISP neck and that such movement is required for the bc_1 catalysis. During the bc_1 catalysis, in order to transfer electrons, the ISP head domain has to move between the cyt. *b* and cyt. c_1 interface under two conformations, the "*b*" and "c_1" positions, respectively (33). When the ISP head domain was fixed at the "*b*" (33) or "c_1" (34) position by an inter-subunit disulfide, which was formed by an engineered cysteine pair between cytochrome *b* or cytochrome c_1 and the head domain of ISP from the *R. sphaeroides* bc_1 complex, the protein showed little electron transfer activity. However, the complex recovers most of its activity upon β-mercaptoethanol treatment, which can release the ISP head domain from the "*b*" position or "c_1" position. Although the movement of the ISP head domain is required for the bc_1 catalysis, the driving force for this movement is still unknown. Brandt proposed the "catalytic switch" mechanism (35) to explain the movement of the ISP head domain. When the iron-sulfur cluster and heme

b_L are in the oxidized form, the ISP head domain remains at the "*b*-position," and the Q cycle starts. QH_2 at the Q_P pocket transfers the first electron to the iron-sulfur cluster, which triggers the head domain to move to the "c_1-position," at which point the iron-sulfur cluster is oxidized by heme c_1, heme b_L is reduced by semiquinone simultaneously. Reduced heme b_L transfers the electron to heme b_H, which triggers the head domain back to the "*b*-position". Then reduced heme c_1 and heme b_H are oxidized by electron carriers cytochrome *c* and Q/QH at the Q_N pocket, respectively. On the other hand, our group suggested that the electron transfer from heme b_L to heme b_H is the driving force for the head domain of ISP to move from the "*b*" position to "c_1" position (36, 37). This suggestion is based on the observation that the two mutations lacking heme b_L and heme b_H show a much slower cytchrome c_1 reduction than that of the wild type .

Inhibitors of the cytochrome bc_1 complex (Figure 9, page 21) – Inhibitors of the cytochrome bc_1 complex are classified into three classes based on their binding sites (38-40, Table 2). Class P inhibitors, also called class I, bind to or near the Q_P site and block the oxidation of ubiquinol or block the electron transfer between the ISP and cytochrome c_1; Class N inhibitors, also called class II, bind to the Q_N site and block the electron transfer between heme b_H and ubiquinone; class PN inhibitors target both sites. Based on the chemical characteristics of the inhibitors and the biophysical effects of heme *b* and the iron-sulfur cluster on the binding of inhibitors, class P inhibitors can be further divided into three sub-groups (Ia, Ib, Ic). Myxothiazol and β-methoxyacrylate stilbene (MOAS), the class Ia inhibitors, block electron transfer from ubiquinol to ISP, containing a common MOA toxophore or its derivatives. The class Ib inhibitor, stigmatellin, blocks the electron transfer from ISP to cytochrome c_1. The class Ib inhibitors contain a

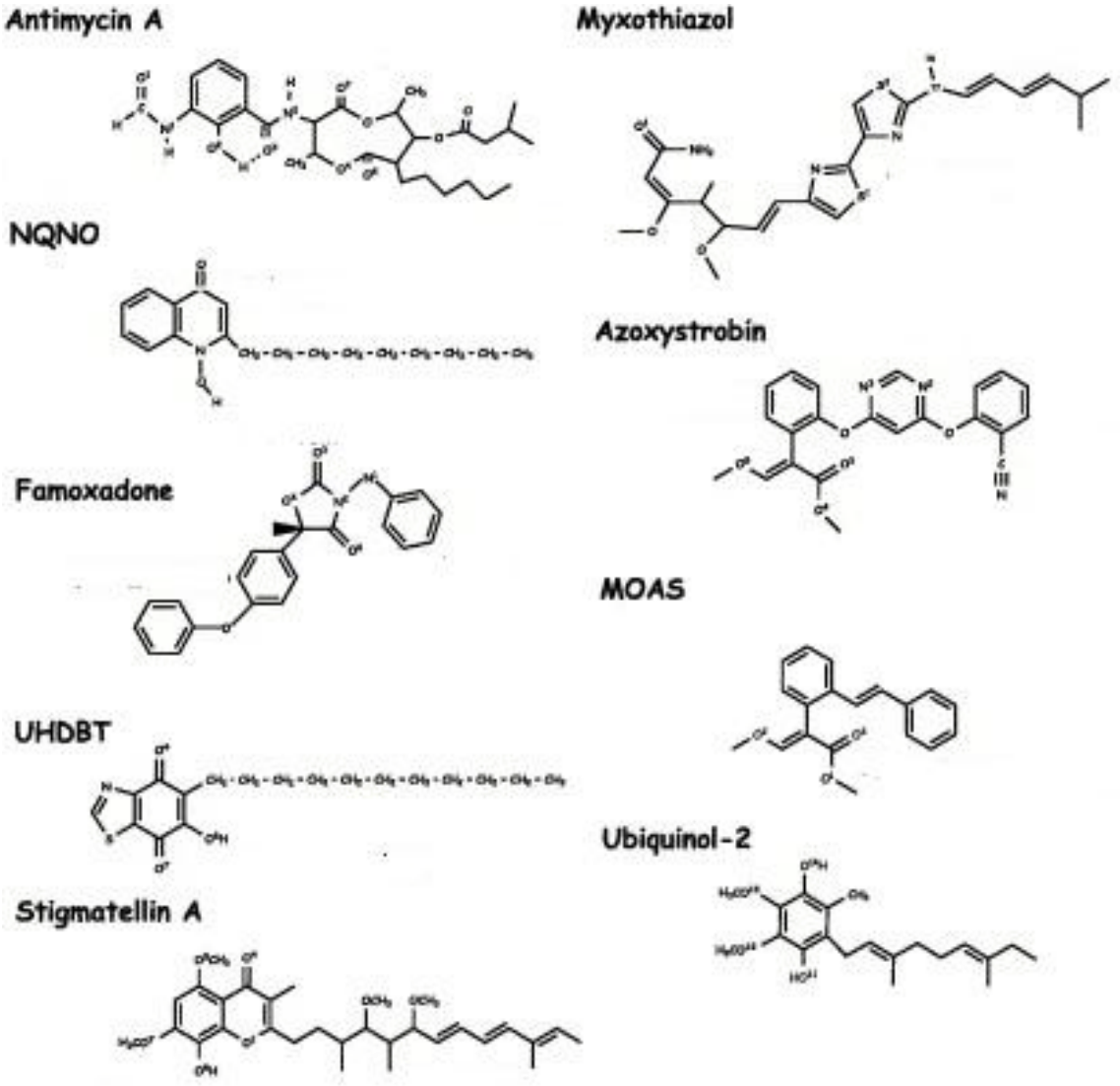

Figure 9. **Chemical structures of cytochrome bc_1 inhibitors (41).**

Table 2. **Classification of cytochrome bc_1 inhibitors.**

Class	subgroup		representative inhibitors
P (Q_P site)	Pm	Ia	Myxothiazol, MOAS
	Pf	Ib	Stigmatellin
	Pf	Ic	UHDBT
N (Q_N site)			Antimycin A, diuron
PN (Q_P and Q_N)			NQNO, funiculosin

NQNO: 2-*n*-nonyl-4-hydroxyquinoline *N*-oxide;
MOAS: methoxyacrylate-stilbene;
UHDBT: 5-undecyl-6-hydroxy-4,7-dioxobenzothiazole;

chromone ring system. The binding of the class Ib inhibitors results in a significant increase of the redox potential of ISP and a changed EPR spectrum of ISP. Meanwhile, it can cause a red-shift of the reduced heme b_L spectrum. Class Ic inhibitors include 2-hydroxy quinone analogues. They can only cause a slight increase of the redox potential of ISP. Class P inhibitors also can be classified into two subgroups, P_m and P_f, based on their ability to induce mobile or fixed conformations of the Rieske ISP (41). P_m class inhibitors like myxothiazol and MOAS induce a dramatic increase in the mobility of the ISP head domain. Upon the binding of P_m inhibitors, the EPR spectrum and redox potential of ISP remain the same. Stigmatellin and UHDBT, which belong to the P_f class, reduce the mobility of the ISP head domain. Upon the binding of the P_f inhibitors, the EPR spectrum and the redox potential of ISP will change. Antimycin A and diuron belong to the class N inhibitors. Class PN inhibitors consist of NQNO and funiculosin (41).

Study system – *Rhodobacter sphaeroides* is an anoxygenic, non-sulfur, purple photosynthetic bacterium. Under anaerobic conditions in the presence of light, the cell grows photoheterotropically (Figure 3A, page 7). Under aerobic conditions in the dark, the cells grow aerobically. The cytochrome bc_1 complex is not an essential component since the electrons from ubiquinol can be transferred to oxygen via a quinol oxidase as an alternative electron transfer pathway (see Figure 3B, page 7). Under semi-aerobic conditions in the dark (Figure 3C, page 7), the cells synthesizes all the components used for photosynthetic growth.

The cyt. bc_1 complex from *R. sphaeroides* has been used as a model system for the study of this complex for the following reasons: (i) This bacterial complex is

functionally analogues to the mitochondrial complex (42). (ii) The *R. sphaeroides* cytochrome bc_1 complex has a simpler protein subunit composition as that of the bovine complex. All bc_1 complexes from different species have 3 core catalytic redox-group-containing subunits: cytochrome *b*, cytochrome c_1, and iron-sulfur protein (ISP). The others are referred to as supernumerary subunits. This bacterial complex has only 4 protein subunits, 3 core subunits, and one supernumerary subunit, which is subunit IV (43), while the bovine complex has 11 protein subunits, 3 core subunits, and 8 supernumerary subunits. This composition of subunits makes *R. sphaeroides* a good system to use for studying the bc_1 complex, especially the supernumerary subunit. (iii) It is possible to express mutant bc_1 complex in *R. sphaeroides.* In eukaryotic systems, such as yeast, the cytochrome *b* is encoded in the mitochondria, so it is inconvenient for site-directed mutagenesis. In *R. sphaeroides*, the three core catalytic subunits are encoded by genes organized in an fbcFBC operon. The subunit IV is encoded by a gene called fbcQ, which is approximately 278kb away from the fbcFBC operon. *R. sphaeroides* strains lacking the fbcFBC operon (BC17) and fbcQ (RSΔIV) have been generated and characterized. A low copy number plasmid, pPKD418, containing the fbcFBCQ genes, with six consecutive histidine residues on the C-terminus of the cyt. c_1 gene (fbcC) (27), facilitates the purification of the wild-type and site-directed mutant bc_1 complex by using the nickel-nitrilotriacetic acid (Ni-NTA) agarose column. (iv) Because the bc_1 complex is not essential for cell aerobic growth (Figure 3B, page 7), it is possible to express a defective mutated bc_1 complex in *R. sphaeroides* under semi-aerobic condition in the dark (44-46). In contrast, eukaryotes cannot survive with a defective bc_1 complex.

Recently, a high resolution (2.35 Å) X-ray crystal structure of the inhibitor loaded three-subunit core complex from *R. sphaeroides* has been available (47). Subunit IV is dissociated from the core complex during crystallization of a four-subunit mutant complex with an arginine substitution at the S-287 of cytochrome *b* and a cysteine substitution at the V-135 of ISP [S287R(cyt. *b*)/V135S (ISP)] (48). Bacterial core subunits are larger than their counterparts in the beef complex. Sequence alignments reveal four extra fragments in the bacterial cytochrome *b* and one each in cytochrome c_1 and ISP. The 3-D structure of the *R. sphaeroides* core complex (47) provides detailed structural information for these extra fragments and supports our suggestion that these extra fragments interact with some parts of their own subunit or their neighboring subunits to stabilize the complex structure (49-52). However, the lack of subunit IV greatly undermined the application value of this bacterial complex structure, especially for the study of supernumerary subunits in the bc_1 complex.

To bridge this gap, we modeled the structure of subunit IV into three-subunit core complex (53, Figure 10 below) using coordinates from subunit 7 of the bovine mitochondrial complex because these two proteins have been identified as small molecular weight Q-binding subunits in their respective complexes by photo affinity labeling studies (54).

Previous study on subunit IV of Rhodobacter sphaeroides bc_1 complex – The bc_1 complex from *Rhodobacter sphaeroides* has been purified and characterized, and the complex is found to contain four subunits (55). Subunit IV of *R. sphaeroides* is an integral subunit of this bacterial complex. The essentiality of subunit IV has been proven

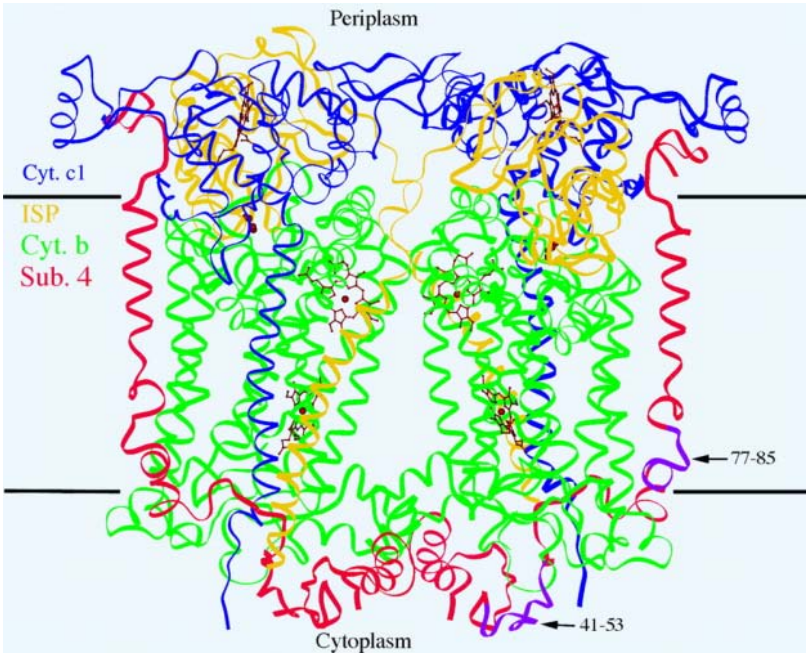

Figure 10. **Ribbon structure of *R. sphaeroides* bc_1 complex.** The three core subunits: cytochrome *b*, cytochrome c_1, and ISP are X-ray crystal structure with a resolution of 2.3 Å. The structure of subunit IV was modeled into the three-subunit core complex (53).

by immuno-chemical studies and genetic approaches (43). All of the four subunits were absorbed by the affinity column coupled with the antibody against subunit IV.

The gene for subunit IV (*fbcQ*) has been cloned and sequenced (56). The *fbcQ* gene is at least 3 kb away from the *fbc* operon which encodes three other core subunits. The subunit IV gene is 372 base pairs long and encodes 124 amino acid residues. The molecular weight of subunit IV is 14384 Da. Based on the hydropathy analysis, fragments from residues 86 to 109 are predicted as a transmembrane helix, as shown in Figure 11 (53, pg 28). The C-terminal and N-terminal of subunit IV have been indicated, through biochemical studies, to be on the periplasmic side (positive side) and the cytoplasmic side (negative side), respectively (53). Although studies of subunit IV can be approached through either the in vivo gene implant or the in vitro reconstituting methods, we have decided to take the latter approach to avoid a large deletion resulting in structural changes and proteins being unable to be expressed. In order to use the in vitro reconstitution method, we need to have a functional, active three-subunit core complex and a subunit IV. The three-subunit core complex is purified from RS ΔIV containing a pRKD418 fbcFBC$_H$ plasmid (57). The subunit IV protein is over-expressed in *E. coli* cells as a glutathione-S-transferase (GST) fusion protein using the expression vector, pGEX/RSIV (58). The recombinant subunit IV is purified from the cell extracts by a procedure involving glutathione agarose gel followed by thrombin digestion and HPLC column chromatography. The addition of purified recombinant IV to the three-subunit core complex, which has a fraction (25%) of the electron transfer activity of the wild-type complex, restores electron transfer activity to that of the wild-type complex (58). Activity restoration requires subunit IV to first be incorporated into the complex through its

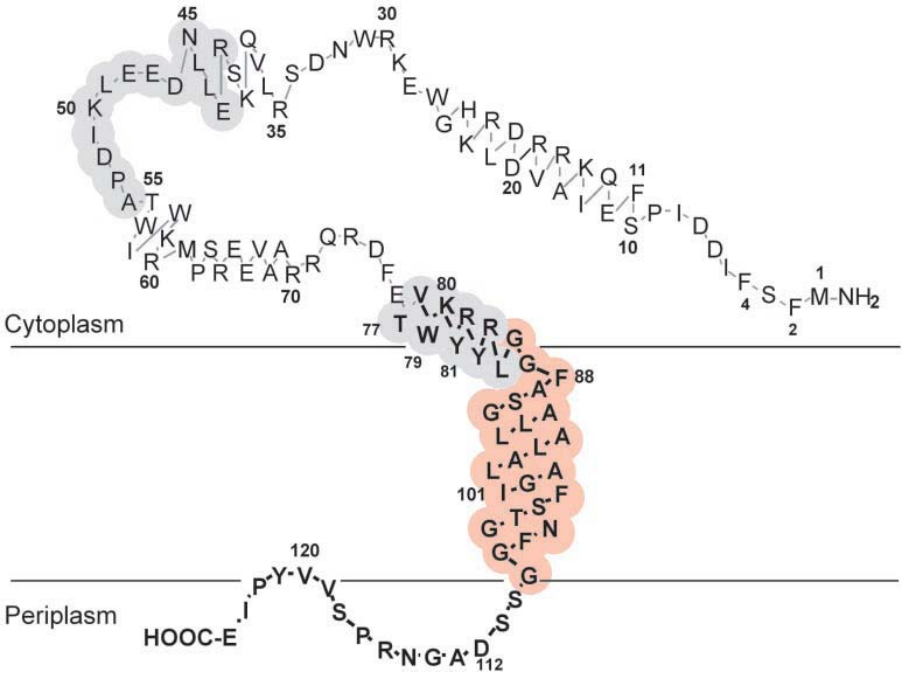

Figure 11. **Localization of interacting regions in the proposed structural model of subunit IV in the chromatophore membrane.**

transmembrane helix region (residues 86-109), and then to interact with the core subunits through residues 41–53 and 77–85, which are on the cytoplasmic side of the membrane and close to the DE loop and helix G of cytochrome *b*, respectively (53).

Superoxide anion radical generation by the cyt. bc_1 complex – A number of toxicities are mediated by mechanisms collectively named "oxidative stress." In the oxidative stress mechanism reactive oxygen species (ROS) interact with cellular constituents, including DNA/RNA, proteins, carbohydrates, and unsaturated lipids, causing irreversible damage to these constituents. Acute exposure to reactive oxygen species can inactivate the iron-sulfur clusters of complexes I, II, and III in the mitochondria electron transport chain, resulting in the stopping of mitochondrial respiration (59). Cumulative oxidative damage has been implicated in a number of disease states, e.g. the aging process, cancer, inflammation, and ischemia-reperfusion injury (60-64). ROS can be either reactive radicals, such as hydroxyl or superoxide, or reactive non-radical species, such as singlet oxygen, peroxynitrite, and peroxide (organic or hydrogen peroxide). Mitochondria have long been considered the major site of intracellular reactive oxygen radical generation (65, 66). During the process of electron transport, about 1-2% of oxygen consumption is not involved in oxidative phosphorylation, but rather in the formation of the superoxide anion (67). Complex I and complex III are the main sites for the superoxide production (68). In complex I, the flavin radical and the ubiquinone radical are the electron donors of the superoxide generation. While in the cyt. bc_1 complex, the ubisemiquinone radical at the Q_P site (69) and the reduced heme b_{566} (or b_L) (70) are suggested as the autoxidizable factors causing superoxide production during bc_1 complex catalysis.

The generation of superoxide anion could decrease if the ubisemiquinone at the Q_P site or the reduced heme b_L are well protected from contact with oxygen. Previous studies indicate that the electron transfer activity of the three-subunit cytochrome bc_1 core complex from *R. sphaeroides* has only one fourth that of the wild type enzyme (57). Addition of subunit IV, the only supernumerary subunit of the *R. sphaeroides* cyt. bc_1 complex, to the core complex restores the activity to the same level as that of the wild type. Subunit IV may prevent electron leakage. In this study, the effect of subunit IV on superoxide generation is discussed. Furthermore, the reaction mechanism of superoxide generation by the cytochrome bc_1 complex is discussed.

References

1. Hatefi, Y. (1985) *Annu. Rev. Biochem*. **54**, 1015-1069
2. Zhang, L., Li, Z., Quinn, B., Yu, L., and Yu, C.A. (2002) *Biochim. Biophys. Acta.* **1556**, 226-232
3. Mitchell, P (1961) *Nature **191**: 144–148*
4. Trumpower, B. L., and Gennis, R. B. (1994) *Annu. Rev. Biochem.* **63**, 675-716
5. Ljungdahl, P. O., Pennoyer, J. D., Robertson, D. E., and Trumpower, B. L. (1987) *Biochimica et Biophysica Acta* . **891**, 227
6. Tso, S.-C., Shenoy, S. K., Quinn, B. N., and Yu, L. (2000) *J. Biol. Chem.* **275**, 15287-15294
7. Trumpower, B. L. (1990) *J. Biol. Chem.* **265**, 11409-11412
8. Erecinska, M., Chance, B., Wilson, D. F., and Dutton, P. L. (1972) *Proc. Natl. Acad. Sci. U.S.A.* **69**, 50-54
9. Mitchell, P. (1976) *J. Theor. Biol.* **62**, 327-367
10. Zhu, J., Egawa, T., Yeh, S. R., Yu, L. and Yu, C. A. (2007) *Proc. Natl. Acad. Sci.* **104**, 4864-4869.
11. Cape, J. L., Bowman, M.K., Kramer, D.M. (2007) *Proc. Natl. Aca. Sci.* **104**, 7887-7892
12. Yu, C.A., Nagoaka, L., Yu, L., and King, T.E. (1978) *Biophys. Res. Commun*. **82**, 1070-1073
13. Slater, E.C. (1973) *Biochim. Biophys. Acta.* **301**, 129-154
14. De Vires, S., Albracht, S.P.J., Berden, J.A., and Slater, E.C. (1981) *J. Biol. Chem.* **256**, 11996-11998

15. Brand, M. D., Reynafarje, B. and Lehninger, A. L. (1976) *J. Biol. Chem*. **251,** 5670-5675

16. Xia, D., Yu, C.-A., Kim, H., Xia, J.Z., Kachurin, A.M., Zhang, L., Yu, L. and Deisenhofer, J. (1997) *Science*, **277**, 60-66

17. Zhang, Z.L., Huang, L.S., Shulmeister, V.M., Chi, Y.I., Kim, K.K., Huang, L.W., Crofts, A.R., Berry, E.A., and Kim, S.H. (1998) *Nature*, **392**, 677-684

18. Hunte, C., Koepke, J., Lange, C., Rossmanith, T., and Michel, H. (2000) *Structure Fold. Des.* **8**, 669-684

19. Lange, C., and Hunte, C. (2002) *Proc. Natl. Acad. Sci. USA* **99** (5), 2800-2805

20. Iwata, S., Lee, J.W., Okada, K., Lee, J.K., Iwata, M., Ramussen, B., Link, T.A., Ramaswamy, S., and Jap, B.K. (1998) *Science*, **281**, 64-71

21. Xia, D., Esser, L., Yu, L., and Yu, C.-A. (2007) *Photosynth. Res*. **92** ,17-34.

22. Gao, X., Wen, X., Esser, L., Quinn, B., Yu, L., Yu, C., and Xia, D. (2003) *Biochemistry* **42**, 9067-9080

23. Ohnishi, T. H., Schagger, H., Meinhardt, S. W., Lobrutto, R., Link, T. A., and von Jagow, G. (1989) *J. Biol. Chem.* **264**, 735-744

24. Gong, X., Yu, L., Xia, D. and Yu C. A. (2005) *J. Biol. Chem*. **280**, 9251-9257

25. Link, T. A., and Iwata, S. (1996) *Biochimica et Biophysica Acta.* **1275**, 54-60

26. Xiao, K., Chandrasekaran, A., Yu, L., and Yu, C. A. (2001) *J. Biol. Chem.* **276**,46125-46131

27. Tian, H., Yu, L., Michael, W., and Yu, C. -A. (1998) *J. Biol. Chem.,* **273**, 27953-27959

28. Xiao, K., Yu, L., and Yu, C. -A. (2000) *J. Biol. Chem.* **275**, 38597-38604

29. Darrouzet E, Valkova-Valchanova M, Christopher, C., Moser, P., Dutton, L, and Daldal, F. (2000) *Proc. Natl. Acad. Sci. U.S.A.* **97**, 4567-4572

30. Nett, J. H., Hunte, C., Trumpower, B. L. (2000) *Eur. J. Biochem.* **267**, (577-5782)

31. Zhang, Z. L., Huang, L-S., Shulmeister, V.M., Chi, Y-I., Kim, K. K., Huang,, L-W., Crofts, A. R., Berry, E. A., and Kim, S-H. (1998) *Nature* **392**, 677-684

32. Kim, H., Xia, D., Yu, C. -A., Kachurin, A., Zhang, L., Yu, L., and Deisenhofer, J. (1998) *Proc. Natl. Acad. Sci. U.S.A.* **95**, 8026-8033

33. Xiao, K., Yu, L., and Yu, C.-A. (2000) *J. Biol. Chem.* **275**, 38597-38604

34. Ma, H. W., Yang, S., Yu, L., and Yu, C.-A. (2008) *Biochimica et Biophysica Acta.* **1777**(3), 317-26.

35. Brandt, U. (1998) *Biochimica et Biophysica Acta* **1365**, 261-268

36. Cen, X., Yu, L., Yu, C.-A. (2008) *FEBS Lett.* **582**, 523-6.

37. Yang, S., Ma, H. W., Yu, L., Yu, C.-A. (2008) *J. Biol. Chem.* **283**,28767-76

38. Link, T. A., Haase, U., Brandt, U., and Jagow, G. (1993) *Journal of Bioenergetics and Biomembranes* **25**, 221-232

39. Von Jagow, G., and Link, Th. A. (1986) *Methods Enzymology* **126**, 253-271

40. Geier, B. M., Haase, U., and Von Jagow, G. (1993) *biol. Soc. Trans* **22**, 203-209

41. Esser, L., Quinn, B., Li, Y.-F., Zhang, M., Elberry, M., Yu, L., Yu, C.-A., and Xia, D. (2004) *Journal of Molecular Biology* **341**, 281

42. Snyder, C., and Trumpower, B. L. (1998) *Biochim. Biophys. Acta* **1365**, 125-134

43. Yu, L., Yu, C.A. (1991) *Biochemistry* **30**, 4934-4939.

44. Knaff, D. B., (1990) T*rends Biochem. Sci*. **15**, 289-291

45. Gennis, R. B., Barquera, B., Hacker, B., van Doren, S. R., Arnaud, S., Crofts, A. R., Davidson, E., Gray, K. A., and Daldal, F. (1993) *J. Bioenerg. Biomembr.* **25**, 195-209

46. Thöny-Meyer, L. (1997) *Microbiol. Mol. Biol. Rev.* **61**, 337-376

47. Esser, L., Elberry, M., Zhou, F., Yu, C. A., Yu, L., Xia, D.(2007) *J. Biol. Chem.* **283,** 2846–2857

48. Elberry, M., Xiao, K., Esser, L., Xia, D., Yu, C. A., Yu, L.(2006) *Biochim. Biophy. Acta*. **1757**, 835-840

49. Xiao, K. H., Yu, C. A., and Yu, L. (2004) *Biochemistry* **43**, 1488-1495

50. Liu, X., Yu, C. A., Yu, L.(2004) *J. Biol. Chem.* **279,** 47363–47371

51. Elberry, M., Yu, L., Yu, C.A. (2006) *Biochemistry*. **45**, 4991-4997

52. Gong, X., Yu, L., and Yu, C.A. (2006) *Biochemistry*. **45**, 11122-11129

53. Tso, S. C., Shenoy, S. K., Quinn, B. N., and Yu, L. (2000) *J. Biol. Chem.* **275** ,15287–15294.

54. Yu, L., and Yu, C.A.(1987) *Biochemistry.* **26**, 3658-3664

55. Yu, L., Mei, Q. C., and Yu, C. A. (1984) *J Biol Chem* **259**, 5752-5760

56. Usui, S., and Yu, L. (1991) *J Biol Chem* **266**, 15644-15649

57. Chen, Y. R., Usui, S., Yu, C. A., and Yu, L. (1994) *Biochemistry* **33**, 10207-10214

58. Chen, Y. R., Yu, C. A., and Yu, L. (1996) *J Biol Chem* **271**, 2057-2062

59. Raha, S., and Robinson, B. H. (2000) *Trends Biochem Sci* **25**, 502-508

60. Shigenaga, M. K., Hagen, T. M., and Ames, B.N. (1994) *Proc. Natl. Acad. Sci. U.S.A.* **91**, 10771-10778

61. Sadek, H. A., Nulton-Person, A. C., Szweda, P. A., and Szweda, L. I.(2003) *Arch. Biochem. Biophys.* **420**, 201-208

62. Lesnefsky, E. J., and Hoppel, C. L. (2003) *Arch. Biochem. Biophys.* **420**, 287-297

63. Moro, M. A., Almeida, A., Polanos, J. P., and Lizasonain, L. (2005) *Free Radical Biology & Medicine* **39**, 1291-1304

64. Petrosillo, G., Ruggiero, F. M., Pistolese, M., and Paradies, G. (2001) *FEBS lett.* **509**, 435-438

65. Loschen, G., Azzi, A., Flohe, L.(1973) *FEBS Lett.* **33** , 84–88.

66. Nohl, H., Hegner, D. (1978) *Eur. J. Biochem.* **82,** 563–567.

67. Boveris, A., Oshino, N., and Chance, B. (1972) *Biochem J* **128**, 617-630

68. Turrens, J. F., A. Boveris, A.(1980) *Biochem. J.* **191**, 421–427.

69. Turrens, J. F., Alexandre, A., and Lehninger, A. L. (1985) *Arch Biochem Biophys* **237**, 408-414

70. Nohl, H., and Jordan, W. (1986) *Biochem Biophys Res Commun* **138**, 533-539

CHAPTER II

IDENTIFICATION OF AMINO ACID RESIDUES ESSENTIAL FOR RECONSTITUTIVE ACTIVITY OF SUBUNIT IV OF THE CYTOCHROME bc_1 COMPLEX FROM RHODOBACTER SPHAEROIDES

Shih-Chia Tso, Ying Yin, Chang-An Yu, and Linda Yu

Biochimica et Biophysica Acta-Bioenergetics (2006)1757, 1561-1567

Introduction

A His-tagged, three-subunit core complex, which is prepared from the chromatophores of a subunit IV-lacking *R. sphaeroides* (RSΔIV) (1) harboring fbc*FBC*$_H$ genes (2) in a low copy number plasmid, pRKD 418, by a method involving dodecylmaltoside solubilization followed by Ni-NTA affinity column chromatography, contains only three subunits, cytochromes *b* and c_1, and the Rieske iron-sulfur protein (2). This three-subunit core complex has a fraction (25%) of the wild-type bc_1 complex activity.

Subunit IV was over-expressed in *Escherichia coli* as a glutathione-S-transferase (GST) fusion protein using the pGEX/RSIV expression vector (3). Recombinant GST-IV fusion protein is purified from cell extracts with glutathione agarose gel. Purified recombinant subunit IV is obtained by thrombin digestion of the fusion protein followed by gel filtration to remove uncleaved fusion protein and thrombin. The addition of purified recombinant subunit IV to the His-tagged, three-subunit core complex restores

enzymatic activity to the same level of wild-type complex (3), indicating that both the three-subunit core complex and the recombinant subunit IV are reconstitutively active, and the recombinant subunit IV can be properly assembled into the bc_1 complex. This success enables us to study the interactions between supernumerary and core subunits, using native or mutated subunit IV, by *in vitro* reconstitution.

By generation and characterization of C-terminal and N-terminal truncated subunit IV mutants, three regions of subunit IV, residues 41-53 (domain I), 77-85 (domain II), and 86-109 (domain III), were identified as essential for interaction with the core complex to restore the bc_1 activity (2). Reconstitutive activity of subunit IV is believed to require interaction of domains I and II with the core complex after it is incorporated into the complex through domain III, which is the only transmembrane helix in the proposed model of subunit IV; this is constructed based on the hydropathy plots of its amino acid sequence (4). This suggestion is based on the observation that subunit IV mutants lacking domain III cannot incorporate into the bc_1 complex, while domain III alone can associate with the core complex but does not restore bc_1 activity (2).

Although deletion mutation studies have identified domains I and II as being required for reconstitutive activity of subunit IV, confirmation with substitution mutation is needed because the loss of activity observed for subunit IV mutants lacking these two domains may result from improper protein assembly or folding due to a large deletion and not from the essentiality of these two regions for activity. We have generated and characterized two subunit IV mutants with alanine substitution at domains I and II to unambiguously establish the region(s) required for interaction with the core subunit to restore bc_1 activity. After the region(s) was(were) established we generated and

characterized subunit IV mutants with single or multiple alanine substitution in the identified region(s) to identify essential residues. We also investigated the mode of interaction between subunit IV and the core complex and the effect of that interaction on the structural stability of the bc_1 complex.

Experimental Procedures

Materials – Dodecylmaltoside (DM) was purchased from Anatrace. The Ni-NTA resin used for purification of the His_6-tagged cytochrome bc_1 complex was from Qiagen. The glutathione-agarose gel was from Sigma. The R408 helper phage, pSELECT-1 vector, BMH 71-18 *mut*S, and JM 109 *Escherichia coli* strains used in the Altered Sites mutagenesis system were from Promega. The *PfuTurbo* DNA polymerase, *Dpn* I, and XL1-Blue *E. coli* strain used in the QuickChange mutagenesis system were from Stratagene. Restriction endonucleases and other DNA-modifying enzymes were purchased from Promega, Life Technologies, Inc., Stratagene, and New England Biolab. The expression vector pGEX-2T and Superdex 200 FPLC column were from Pharmacia. Primers and oligonucleotides were synthesized by the DNA/Protein Core Facility of Oklahoma State University. 2,3-Dimethoxy-5-methyl-6-geranyl-1, 4-benzoquinol (Q_2H_2) was synthesized in our laboratory as previously described (5).

Growth of bacteria – *E. coli* cells were grown at 37 ˚C in LB medium. Extra-rich medium (TYP) was used in procedures for the rescue of single-stranded DNA. For photosynthetic growth of the plasmid-bearing *R. sphaeroides* cells, an enriched Siström medium containing 5 mM Glutamate and 0.2% casamino acids was used (6). Antibiotics were added to the following concentrations: ampicillin, 100-125 mg/liter; tetracycline,

10-15 mg/liter for *E. coli* and 1 mg/liter for *R. sphaeroides*; kanamycin sulfate, 30-50 mg/liter for *E. coli* and 20 mg/liter for *R. sphaeroides*; and trimethoprim, 25 mg/liter for *R. sphaeroides*.

Generation of R. sphaeroides strains expressing his-tagged, four-subunit, and three-subunit cytochrome bc_1 complexes – The expression vector for the His-tagged, wild-type, four-subunit cytochrome bc_1 complex (pRKD*fbc*FBC_HQ) (6) and the subunit IV deficient, three-subunit core complex (pRKD*fbc*FBC_H) (2) were constructed as previous described. pRKD*fbc*FBC_HQ and pRKD*fbc*FBC_H were mobilized into BC17 and RSΔIV, respectively, by parental conjugation (7) to generate pPRKD *fbc*FBC_HQ/BC17 and pRKD*fbc*FBC_H /RSΔIV, for expressing His-tagged four-subunit and three-subunit complexes, respectively.

Preparations and assay of His_6-tagged cytochrome bc_1 complexes – The His_6-tagged, four-subunit, wild-type complex and three-subunit core complex, were purified from chromatophores of photosynthetically grown pRKD*fbc*FBC_HQ/BC17 (6) and pRKD*fbc*FBC_H /RSΔIV (2) cells, respectively, according to the previously described method.

Cytochrome bc_1 complex activity was assayed as previously reported (6). An appropriate amount of enzyme preparation (1-3 μM cytochrome *b* in 50 mM TriCl, pH 8.0, containing 100 mM NaCl and 0.01% DM) was added to an assay mixture (1 ml) containing 50 mM Na^+/K^+ phosphate buffer, pH 7.4, 1 mM EDTA, 100 μM horse heart cytochrome *c* (from Sigma) and 25 μM Q_2H_2. Activity was determined by measuring the reduction of cytochrome *c* (the increase in absorbance at 550 nm) in a Shimadzu UV-2101PC, at 23 ˚C, using a millimolar extinction coefficient of 18.5 for the calculation.

The non-enzymatic reduction of cytochrome *c by* Q_2H_2, determined under the same conditions in the absence of enzyme, was subtracted from the assay.

Recombinant DNA techniques – Restriction enzyme digestion, large scale isolation and mini-preparation of plasmid DNA, agarose electrophoresis, purification of DNA fragments from gel matrices, and immunological screening of transformants for production of subunit IV mutants with antibodies against subunit IV were performed according to the protocols described by Sambrook *et al*. (8).

Generation of E. coli strains expressing GST-mutated IV fusion proteins – Mutations were constructed by site-directed mutagenesis using either the Altered Sites system from Promega Corp or the QuickChange system from Stratagene. The pGEX/IV and pSelect/IV plasmids were used as templates for the Quick Change mutagenesis system and the Altered sites system, respectively. The mutant oligonucleotides used are summarized in Table 3, pg 41.

The QuickChange system generates mutations by PCR amplifications, which were performed in a minicycler obtained from M. J. Research. The thermal cycle was set-up as follows: (1) 95 °C for 30 sec for initiation; (2) 95 °C for 30 sec for denaturation; (3) decreasing temperature slowly (1 °C every 8 sec) to 55 °C; (4) 55 °C for 1 min for annealing; and (5) 72 °C for 12 min for extension. Steps 2 to 5 were repeated 19 times. The PCR product was treated with *Dpn* I to digest the DNA template and select for the *in vitro* synthesized mutation-containing DNA, because DNA isolated from almost all *E. coli* strains was *dam* methylated and therefore susceptible to *Dpn* I digestion, while the *in vitro* synthesized DNA was not. The *Dpn* I treated product was then transformed into

Table 3. **Oligonucleotides used for site-directed mutagenesis**

IV(41-53)A	(F)*	5’-CGCCTGGTGCAGAAATCG GCCGCGGCCGCCGCCGCCGCGGAACTCAAGATCGATCC-3’
IV(41-53)A	(R)	5’-GGATCGATCTTGAGTTCC GCGGCGGCGGCGGCCGCGGCCGATTTCTGCACCAGGCG-3’
IV(77-85)A	(F)	5’-GAGGCTGCCGCGGCAGCT GCCGCCGCCGCCGGCGGCTTCGCCTCGGGC-3’
IV(77-85)A	(R)	5’-GAGGCTGCCGCGGCAGCT GCCGCCGCCGCCGGCGGCTTCGCCTCGGGC-3’
IV(T77A)	(F)	5’-CCAGCGCGATTTCGAGGCTGTCTGGAAATATCG-3’
IV(T77A)	(R)	5’-CGATATTTCCAGACAGCCTCGAAATCGCGCTGG-3’
IV(V78A)	(F)	5’-CGCGATTTCGAGACTGCCTGGAAATATCGCTAC-3’
IV(V78A)	(R)	5’-GTAGCGATATTTCCAGGCAGTCTCGAAATCGCG-3’
IV(W79A)	(F)	5’-GATTTCGAGACTGTCGCGAAATATCGCTACCGCCTC-3’
IV(W79A)	(R)	5’-GAGGCGGTAGCGATATTTCGCGACAGTCTCGAAATC-3’
IV(K80A)		5’-TTCGAGACTGTCTGGGCATATCGCTACCGCCT-3’
IV(Y81A)	(F)	5’-GAGACTGTCTGGAAAGCTCGCTACCGCCTCGG-3’
IV(Y81A)	(R)	5’-CCGAGGCGGTAGCGAGCTTTCCAGACAGTCTC-3’
IV(R82A)	(F)	5’-CTGTCTGGAAATATGCCTACCGCCTCGGCGG-3’
IV(R82A)	(R)	5’-CCGCCGAGGCGGTAGGCATATTTCCAGACAG-3’
IV(Y83A)		5’-GAAATATCGCGCCCGCCTCGG-3’
IV(R84A)		5’-ATATCGCTACGCCCTCGGCGGCTT-3
IV(81-84)A	(F)	5’-GAGACTGTCTGGAAAGCTGCCGCCGCCCTCGG-3’
IV(81-84)A	(R)	5’-CCGAGGGCGGCGGCAGCTTTCCAGACAGTCTC-3’
IV(L85A)	(F)	5’- GAAATATCGCTACCGCGCCGGCGGCTTCGCCTCG-3’
IV(L85A)	(R)	5’-CGAGGCGAAGCCGCCGGCGCGGTAGCGATATTTC-3’
IV(Y81T)	(F)	5’-GAGACTGTCTGGAAAACTCGCTACCGCCTCGG-3’
IV(Y81T)	(R)	5’-CCGAGGCGGTAGCGAGTTTTCCAGACAGTCTC-3’
IV(Y81F)	(F)	5’-GAGACTGTCTGGAAATTTCGCTACCGCCTCGGC-3’
IV(Y81F)	(R)	5’-GCCGAGGCGGTAGCGAAATTTCCAGACAGTCTC-3’
IV(R82E)		5’-GTCTGGAAATATGAGTACCGCCTCGGCGGCT-3’
IV(R82K)		5’-GTCTGGAAATATAAGTACCGCCTCGGCGGCT-3’
IV(Y83T)	(F)	5’-CTGGAAATATCGCACCCGCCTCGGCGGC-3’
IV(Y83T)	(R)	5’-GCCGCCGAGGCGGGTGCGATATTTCCAG-3’
IV(R84E)	(F)	5’-GTCTGGAAATATCGCTACGAGCTCGGCGGCTTCGCCTCG-3’
IV(R84E)	(R)	5’-CGAGGCGAAGCCGCCGAGCTCGTAGCGATATTTCCAGAC-3’
IV(R84K)	(F)	5’-GTCTGGAAATATCGCTACAAGCTCGGCGGCTTCGCCTCG-3’
IV(R84K)	(R)	5’-CGAGGCGAAGCCGCCGAGCTTGTAGCGATATTTCCAGAC-3’

*The underlined bases correspond to the genetic codes for the amino acid(s) to be mutated.

F and R in the parentheses denote forward and reverse primers, respectively.

XL1-Blue competent cells. Plasmid purified from a single XL1-Blue colony was sequenced to confirm the mutation and then transformed into *E. coli* KS1000 cells.

Isolation of recombinant wild-type and mutants subunit IVs – Production of GST-IV or GST-IVm fusion protein by *E. coli* KS1000 carrying pGEX/RSIV or pGEX/RSIVm was essentially the same as that described previously (3) with modifications. 250-ml of overnight grown cultures with OD_{600nm} = 0.6-0.8 were used to inoculate 6-L of LB broth containing 125 µg/ml ampicillin and 2% glucose. The resulting culture was incubated at 23 ˚C with vigorous shaking. When OD_{600nm} of the culture reached 1.0 (usually 12-14 hours from inoculation), IPTG was added to a final concentration of 0.2 mM, and grown at 23 ˚C for 6 hrs before being harvested by centrifugation at 8,000 xg for 30 min. About 30-35 g cells were obtained and resuspended in 100 ml of 12 mM Na/K phosphate, pH 7.3, containing 140 mM NaCl and 2.7 mM KCl (PBS).

Cells were broken in a French press at 1000 p.s.i. During French pressing, PMSF (500 mM in DMSO) was added to the cell suspension to a final concentration of 1 mM. Triton X-100 was added to the broken cell suspension for a final concentration of 1 %. The suspension was stirred for 30 min at 0 ˚C and centrifuged at 40,000 x g for 20 min. The supernatant was mixed with 15 ml of glutathione-agarose gel equilibrated with PBS. This gel mixture was shaken gently for 30 min at room temperature and then packed into a column (1.6 cm x 20 cm). The column was washed with PBS until the $OD_{280\ nm}$ of the effluent was less than 0.01 before the GST/subunit IV fusion protein was eluted from the column with 10 mM glutathione in 50 mM Tris-HCl, pH 8.0. The fusion protein containing fractions were collected and concentrated to a protein concentration of 10

mg/ml by Centriprep-10. The fusion protein was treated with thrombin (1 NIH unit/1 mg fusion protein) at room temperature for 2 hrs to release subunit IV from GST. The thrombin-digested sample was dialyzed against one liter of PBS buffer at 4 ˚C, overnight, with three changes of the buffer, to remove the glutathionine. The dialyzed sample was first treated with a small amount of glutathione beads to partially remove the released GST, and then subjected to gel filtration with a Superdex-200 FPLC column to completely remove both the GST and thrombin. Purified wild-type and mutant subunit IVs contain no detergent and exist as soluble aggregates. The use of detergent-free subunit IV preparations in the reconstitution study is to avoid complications arising from variable detergent concentrations in the system, since reconstitutive activity of the three-subunit core complex is very sensitive to the detergent concentration used. The detergent present in the core complex is sufficient to disperse subunit IV.

The protein concentration of the purified wild-type subunit IV was estimated by absorbance at 280 nm in the presence of 1% SDS, using a millimolar extinction coefficient of 32.0 cm^{-1}. This extinction coefficient was calculated according to the number of tryptophan (Trp) residues and tyrosine (Tyr) residues in the wild-type subunit IV sequence (5 Trp and 3 Tyr) by the following equation (9):

$$\varepsilon_{280}\ [mM^{-1}cm^{-1}] = 5.50 \times n_{Trp} + 1.49 \times n_{Tyr}$$

For Subunit IV mutants whose composition of tryptophan and tyrosine has been altered, their extinction coefficients were calculated accordingly.

Differential scanning calorimetry (DSC) measurement – Calorimetric measurements were performed in a Nano-DSC II from Calorimetry Sciences Corp. All reference and sample solutions were degassed prior to use. A 0.55 ml of protein sample

(2 mg/ml) was loaded into the sample cell, and the same volume of the buffer was loaded into the reference cell. The sample and the buffer were heated from 10 ˚C to 90 ˚C, cooled back to 10 ˚C, and heated again to 90 ˚C, with the 1 ˚C per min scanning rate for both the heating and the cooling. The cells were equilibrated at 10 ˚C and 90 ˚C for 10 min before the heating and the cooling, respectively. The difference of input heat flow between the sample cell and reference cell was recorded with 6 data-points per ˚C, and plotted as a function of temperature by the data acquisition program DscRun, from the Nano DSC program group. The second heating was used as the baseline for analysis. Transition temperature and enthalpy change of transition were calculated by using the CpCalc program from the Nano DSC program group.

Other biochemical methods – SDS-PAGE were performed by the method of Laemmli (10). Cytochromes *b* (11) and cytochrome c_1 contents (12) were determined as previously described.

Results and Discussions

A region comprising residues 77-85 is essential for reconstitutive activity of subunit IV – Our previous study (2) shows that subunit IV that lacks residues 41-53 or residues 77-85 had a decreased ability in bc_1 activity restoration to the core complex (reconstitutive activity), indicating that these two regions are essential. However, it is a well-known fact that deletion mutations often cause protein to lose its functional activity due to improper assembly or folding and not to the essentiality of the deleted fragment. Therefore, to unambiguously establish the interacting region(s) of subunit IV required for

reconstitutive activity, two subunit IV mutants, one each with alanine substitution at residues 41-53 [IV(41-53)A] and 77-85 [IV(77-85)A], were constructed and characterized.

These two alanine substitution mutants were produced in *E. coli* as GST fusion proteins using the constructed expression vectors pGEX/IV(41-53)A and pGEX/IV(77-85)A, respectively. The yield and purity of these two recombinant GST-mutant IV fusion proteins are comparable to that of GST-wild type IV fusion protein. Purified recombinant subunit IV mutants are obtained from their respective fusion proteins by thrombin cleavage and gel filtration.

The addition of the purified recombinant IV(41-53)A mutant to the three-subunit core complex restores the cytochrome bc_1 complex activity to the same level as that of the recombinant wild-type IV (see Table 4, next page). On the other hand, addition of purified, recombinant IV(77-85)A mutant to the three-subunit core complex restores only 15% of the bc_1 activity (see Table 4, next page). These results indicate that some specific residues at positions 77-85, but not at positions 41-53, are required for reconstitutive activity of subunit IV. The loss of activity previously observed in a subunit IV mutant lacking residues 41-53 (2) must result from improper folding or assembly due to the deletion.

Identification of residues essential for reconstitutive activity of subunit IV – After establishing that residues 77-85 are required for the reconstitutive activity of subunit IV, our next step was to identify the essential amino acid residues in this region (see Figure 12, pg 47). Recombinant subunit IV mutants with alanine substitution at each residue of this region were generated and their maximum reconstitutive activities determined (see Table 4, next page). Mutants IV(V78A), IV(L85A) (T77A), IV(W79A), and IV(K80A) have the same or more than 95% of reconstitutive activity as that of the

Table 4. **Reconstitutive activity of subunit IV mutants**

Subunit IV	Reconstitutive Activity %	Subunit IV	Reconstitutive Activity %
Wild-type IV	100	IV(Y81T)	63
IV(41-53)A	106	IV(Y81F)	83
IV(77-85)A	15	IV(R82E)	56
IV(T77A)	95	IV(R82K)	95
IV(V78A)	105	IV(Y83T)	58
IV(W79A)	98	IV(Y83F)	87
IV(K80A)	97	IV(R84E)	55
IV(L85A)	101	IV(R84K)	100
IV(77-80, 85)A	99	IV(R82, 84E)	55
IV(Y81A)	83	IV(Y81, 83T)	60
IV(R82A)	77	IV(Y81, 83F)	82
IV(Y83A)	80	IV($R_{81}Y_{82}R_{83}Y_{84}$)	22
IV(R84A)	76		
IV(81-84)A	20		

180 µl aliquots of His_6-tagged three subunit core complex, 3.3 µM cytochrome *b*, in 50 mM TrisCl buffer, pH 7,5 containing 100 mM NaCl and 0.01% dodecylmaltoside, were mixed with 20 µl of purified recombinant wild-type and mutant subunit IVs, 60 µM, in 50 mM TrisCl buffer, pH 7.5, containing 100 mM NaCl, 0.01% dodecylmaltoside and 20% glycerol. The mixtures were incubated at 4°C for 1 h before the bc_1 activity was determined. The 100% reconstitutive activity represents the bc_1 activity restoration to the three-subunit core complex upon addition of recombinant, wild-type IV. Every data point is average of at least three repetitions; the deviation between repetitions is less than 2%.

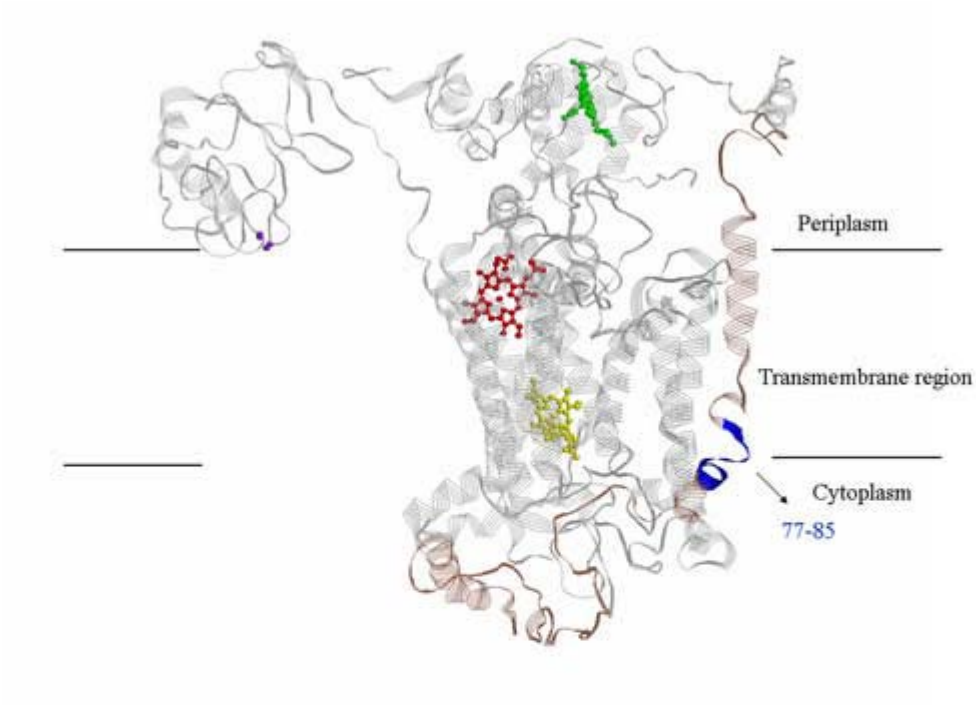

Figure 12. **Location of residues 77-85 of subunit IV in the proposed structural model of the *R. sphaeroides* bc_1 complex.** One monomer of the bc_1 complex is displayed. Subunit IV is brown and residues 77-85 are blue. The three core subunits are shown in gray for clarity. Redox centers are displayed in ball and stick formations: heme b_L - red; heme b_H - yellow; heme c_1 - green; iron-sulfur cluster - purple.

wild-type IV, indicating that these residues are not essential. To further confirm the non-essentiality of these five residues, a mutant with all five residues replaced with alannine, [IV (77-80, 85)A], was generated and characterized. As expected, purified recombinant IV (77-80, 85)A mutant has about 99% of the reconstitutive activity of the wild-type IV (see Table 4, pg 46), confirming their nonessentiality. In contrast, a significant reduction of the reconstitutive activities was observed in mutants IV(Y81A), IV(R82A), IV(Y83A), and IV(R84A). They have, respectively, 83%, 77%, 80%, and 76% of the reconstitutive activity, indicating that these four residues are important. To further confirm the essentiality of these four residues, a subunit IV mutant, in which all of these four residues are replaced with alanine [IV(81-84)A], was constructed and characterized. The IV(81-84)A mutant has 20% of the reconstitutive activity, similar to that observed for the IV(77-85)A mutant (see Table 4). This result not only confirms the requirement of residues 81-84 of subunit IV for activity, but it also suggests that the function of these four residues is additive.

Identification of the functional important groups in residues 81-84 of subunit IV – It has been suggested (2) that the reconstitutive activity of subunit IV involves specific interaction, in addition to physical association, with the core complex through the transmembrane helix (residues 96-109) region of subunit IV. Since residues 81-84, YRYR, are essential for interaction with the core complex to exert reconstitutive activity, it is of interest to see what type of interaction is involved.

R82 and R84 each contain a positively charged side chain, thus their involvement in ionic interaction with the core complex was examined. When R82 and R84 are each replaced with glutamate, the resulting mutant subunit IVs, R82E and R84E, have,

respectively, 56% and 55 % of the reconstitutive activity (see Table 4). On the other hand, when R82 and R84 are each replaced with lysine, the resulting mutants IV (R82K and R84K) have about the same reconstitutive activity as the wild-type IV, indicating that a positively charged side chain in the R82 or R84 of subunit IV is essential; the side chain provides ionic interaction with negatively charged residues in the core subunits. Since an additive mutational effect is observed for alanine substitutions at residues 81-84, it is of interest to see the mutational effect of a mutant with both R82 and R84 substituted with glutamate [IV(R82E, R84E)]. Surprisingly, the double mutant, IV(R82E, R84E) still has 55% of the reconstitutive activity, suggesting that the maximum ionic interaction providing by these two ariginine residues accounts for only about 50% of the reconstitutive activity. The exact interaction partner of these residues will have to wait until the high resolution structure becomes available.

The Y81 and Y83 of subunit IV possess both aromatic and hydroxyl groups. To determine which of these two functional groups are involved, each of the two tyrosine residues was replaced with threonine and phenylalanine and their reconstitutive activity was determined. Mutants IV(Y81T) and IV(Y83T), have, respectively, 63% and 58% of the activity; mutants Y81F and Y83F, have, respectively, 83% and 87% of the activity. These results indicate that both the aromatic and hydroxyl group in Y81 and Y83 are important, but that the aromatic group is more important than the hydroxyl group. It should also be noted that there is no additive mutational effect observed in the mutant where both Y81 and 83 are replaced with either threonine [IV(Y81, 83T)] or phenylalanine [IV(Y81, 83F)]. Double mutants, IV(Y81, 83T) and (Y81, 83F), have, 60% and 82% of the reconstitutive activity, respectively, similar to that of the single threonine

substitution mutants [IV(Y81T) and IV(Y83T)], or to that of the single phenylalanine substitution mutants [IV(Y81F) and IV(Y83F)].

The sequence of $Y_{81}R_{82}Y_{83}R_{84}$ is critical, since when they are changed to $R_{81}Y_{82}R_{83}Y_{84}$, the resulting subunit IV mutant lost about 80% of reconstitutive activity (see Table 4, pg 46).

Residues 81-84 are not essential for the physical association of subunit IV to the three-subunit complex – Since the interaction of subunit IV with the core subunits through residues 81-84 is required for reconstitutive activity, it is important to see whether or not this interaction affects the binding affinity of subunit IV to the core complex. The purified recombinant wild-type and subunit IV mutants: IV(Y81A), IV(R82A), IV(Y83A), IV(R84A), IV(81-84)A, IV(R84E), IV(RYRY) were each incubated with an His-tagged, three-subunit core complex, for 1 hr at 0 ˚C. Three equal volumes of aliquots were withdraw from each mixture, applied to Ni-NTA columns, and washed, respectively, with 10 column volumes of buffers containing 0.01, 0.02, and 0.05% dodecylmaltoside before being eluted with a buffer containing 50 mM histidine.

SDS-PAGE analysis of the column eluates indicates that the amount of wild-type and mutant IV associated with the core complex decreases as the detergent concentration in the washing buffer increases (data not shown). However, the amount of each mutant IV associated with the core complex after a given concentration of detergent wash is comparable to that of the wild-type IV, indicating that these subunit IV mutants associated with the core complex in the same manner as the wild-type IV. In other words, interaction of subunit IV with the core complex through residues 81-84 is required only for reconstitutive activity, not for the association of subunit IV to the core complex. This is

consistent with the previous finding (2) that association of subunit IV to the core complex requires only the transmembrane helix region. However, a possibility exists that the interaction provided by these four residues does affect the binding affinity of subunit IV to the core complex, but it is too small to be detected by the method used. In the other words, the contribution of this region to the physical association of subunit IV to core subunits is weaker than the dissociation of subunit IV from the complex caused by the detergent treatment. Since the subunit IV mutant lacking the transmembrane region has no reconstitutive activity, regardless of how high the concentration of mutant protein used, it is clear that the reconstitutive function of residues 81-84 requires the presence of the transmembrane region to properly bind subunit IV to the core complex.

Residues 81-84 of subunit IV contribute to the structural stability of the cytochrome bc_1 complex – Figure 13 (below) shows differential scanning calorimetric (DSC) thermograms of the three-subunit core complex, four-subunit wild-type complex, and reconstituted complex formed from the three-subunit core complex and recombinant, purified, wild-type IV. The four-subunit wild-type complex undergoes thermodenaturation at a T_m of 46.4 °C with an enthalpy change (ΔH) of 97.6 kcal per mole. When the three-subunit core complex undergoes thermodenaturation, a T_m at 42.1 °C and ΔH of 55.2 kcal per mole is observed. These results indicate that the three-subunit core complex is structurally less stable than the four-subunit wild-type complex.

After the addition of purified, recombinant wild-type IV to the three-subunit core, the resulting complex undergoes thermodenaturation at 46.4 ˚C with a ΔH of 97.4 kcal/mole, similar to values observed for the four-subunit wild-type complex. This result

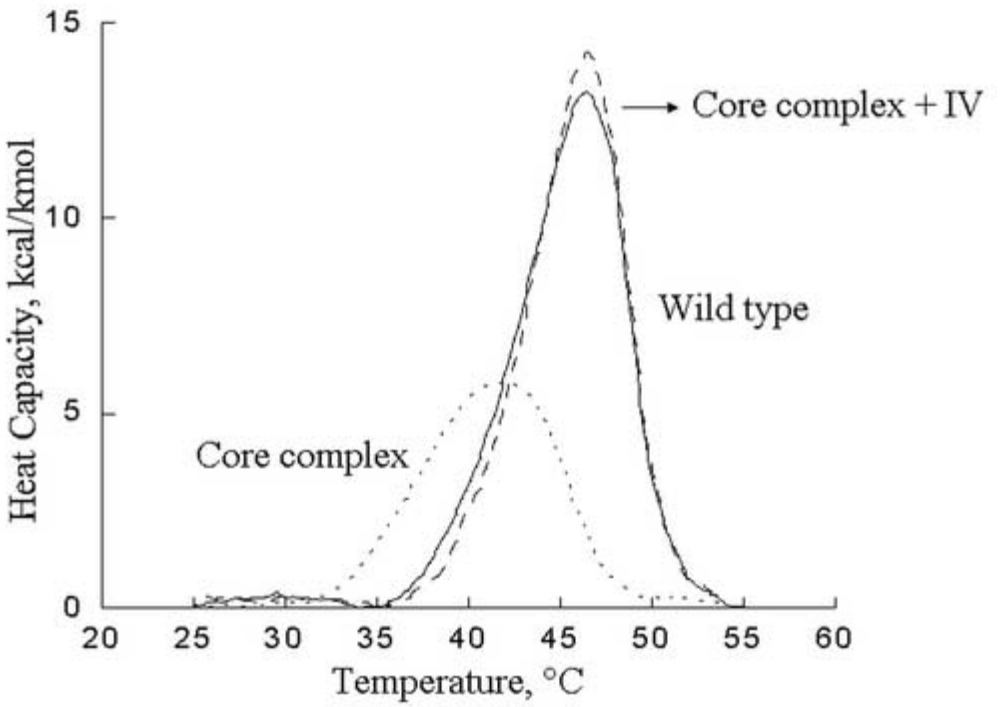

Figure 13. **DSC thermograms of three-subunit core complex, four-subunit wild-type complex, and reconstituted complex formed from the core complex and recombinant, wild-type IV.** The solid curve is the DSC thermogram of His6-tagged, four-subunit, wild-type cytochrome bc_1 complex, 30 μM cytochrome *b*, in 83 mM phosphate, 8 mM TrisCl buffer, pH 7.4, containing 17 mM NaCl, 0.002% DM, and 3.3% glycerol. The curves with dotted lines or broken lines are DSC thermograms of His6-tagged, three-subunit core complex and the complex formed from the His6-tagged core complex and wild-type subunit IV (40 μM), respectively, measured under identical conditions as those for the wild-type complex.

confirms that in the absence of subunit IV, the complex is structurally less stable. However, it is unknown whether structural stability of the bc_1 complex requires just the physical association of subunit IV to the complex or also needs the interaction of subunit IV with the core complex after incorporation into the complex. This can be answered by comparing the thermotropic properties of bc_1 complexes formed from the core complex and the wild-type or subunit IV mutants having mutations at residues 81-84. If association of subunit IV to the complex is required for structural stability, one would expect the reconstituted mutant complexes to have thermotropic properties similar to those of the wild-type. If interaction of subunit IV with the core complex, after incorporation into the complex, is required for structural stability of reconstituted bc_1 complex, one would expect to see a decrease in thermotropic parameters (T_m or ΔH) in the reconstituted complex formed from mutant subunit IV and the core complex.

When reconstituted bc_1 complexes, formed with mutants IV(Y81A), IV(R82A), IV(Y83A), IV(R84A), and IV(81-84)A, are subjected to thermodenaturation, they show, respectively, T_ms at 44.8, 43.7, 44.5, 43.8, and 42.3 ˚C with ΔH of 91.2, 87.2, 89.2, 85.6, and 64.1 kcal/mole (see Table 5, below). They decreased by 1.6, 2.7, 1.9, 2.6, and 4.1 ˚C in their T_m values and by 6.2, 10.2, 8.2, 11.8, and 33.3 kcal/mole in their ΔH values, respectively, compared to the complex formed with wild-type IV. These results indicate that interactions of subunit IV, through residues 81-84, with residues in core subunits increase the structural stability of the bc_1 complex.

Since hydrophobic interaction through phenyl groups at residues Y81 and Y83 and ionic interaction through positively charged groups at R82 and R84 are essential for reconstitutive activity of subunit IV, it is of interest to investigate whether these two types

Table 5. **Thermotropic properties of the bc_1 complexes reconstituted from the core complex and subunit IV mutants.**

The *bc*1 complexes	T_m, °C	ΔH, kcal/mol
Wild type complex	46.4	97.6
Core complex	42.1	55.2
Core complex + wild type IV	46.4	97.4
Core complex + IV(Y81A)	44.8	91.2
Core complex + IV(R82A)	43.7	87.2
Core complex + IV(Y83A)	44.5	89.2
Core complex + IV(R84A)	43.8	85.6
Core complex + IV(81-84)A	42.3	64.1
Core complex + IV(Y81T)	43.6	81.2
Core complex + IV(Y81F)	44.7	91.6
Core complex + IV(R84E)	43.2	78.2
Core complex + IV(R84K)	46.4	97.4

Every data point is average of three samples.

of interactions affect the structural stability of the bc_1 complex. When reconstituted complexes formed with IV(Y81T) and IV(R84E) undergo thermodenaturation, they show T_ms at 43.6 and 43.2 ˚C with ΔHs of 81.2 and 78.2 kcal/mol, respectively, indicating that hydrophobic interaction through the phenyl group at Y81 or Y83 and ionic interaction through the positively charged group at R82 or R84 contribute to the structural stability of the bc_1 complex. Since the reconstituted complex formed with the IV (Y81F) mutant has a higher reconsitutive activity, T_m, and ΔH than that formed with the IV (Y81T) mutant, it is likely that the hydrophobic interaction with the phenyl group at Y81 of subunit IV contributes more to the structural stability of the complex than does the hydrogen bonding provided by the hydroxyl group of this residue. However, this conclusion should be interpreted with caution, since the hydroxyl group on threonine has somewhat different ionization properties (i.e. pKa) than the hydroxyl group on tyrosine. The observation that the complex formed with IV(R84K) mutant has a T_m at 46.4 ˚C and a ΔH of 97.4 kcal/mol, similar to that of the complex formed with the wild-type IV, further confirms the requirement of ionic interaction through the positively charged group in R84 of subunit IV for structural stability of the bc_1 complex.

Summary

Previous studies indicate that a region of subunit IV comprised of residues 77-85 is identified as essential for interaction with the core complex to restore the bc_1 activity (reconstitutive activity). Recombinant subunit IV mutants with single or multiple alanine substitution at this region were generated and characterized to identify the essential amino acid residues. Residues 81-84, with a sequence of YRYR, are required for

reconstitutive activity of subunit IV, because a mutant with these four residues substituted with alanine has little activity, while a mutant with alanine substitution at residues 77-80 and 85 have the same reconstitutive activity as that of the wild-type IV. The positively charged group at R82 and R84 and both the hydroxyl group and aromatic group at Y81 and Y83 are important. The interactions between the four residues of subunit IV and the residues of core subunits are also responsible for the stability of the complex. However, these interactions are not essential for the incorporation of subunit IV into the bc_1 complex.

References

1. Chen, Y. R., Usui, S., Yu, C. A., Yu, L. (1994) *Biochemistry* **33**,10207-10214.
2. Tso, S. C., Shenoy, S. K., Quinn, B. N., Yu, L. (2000) *J. Biol. Chem.* **275**,15287-15294.
3. Chen, Y. R., Yu, C. A., Yu, L. (1996) *J. Biol. Chem.* **271**, 2057-2062.
4. Usui, S., Yu, L. (1991) *J. Biol. Chem.* **266**, 15644-15649.
5. Yu, C. A., Yu, L. (1982) *Biochemistry* **21**, 4096-4101.
6. Tian, H., Yu, L. Mather, M. W., Yu, C. A. (1998) *J. Biol. Chem.* **27**, 27953-27959.
7. Donohue, T. J., McEwan, A. G., Van Doren, S., Crofts, A. R., Kaplan, S. (1988) *Biochemistry* **27**, 1918-1925.
8. Sambrook, J., Fritsch, E. F., Maniatis, T. (1989) Cold Spring Harbor Laboratory Press, Cold Spring Harbor, N.Y.
9. Pace, C. N., Vajdos, F., Fee, L., Grimsley, G., Gray, T. (1995) *Protein Sci.* **4**, 2411-2423.
10. Laemmli, U. (1970) *Nature* **227**, 680-685.
11. Berden, J. A., Slater, E. C. (1970) *Biochim. Biophys. Acta* **216**, 237-249.
12. Yu, L., Doug, J. H., Yu, C. A. (1986) *Biochim. Biophys. Acta* **852**, 203-211.

CHAPTER III

EFFECT OF SUBUNIT IV ON SUPEROXIDE GENERATION BY *RHODOBACTER SPHAEROIDES* CYTOCHROME bc_1 COMPLEX

Ying Yin, Shih-Chia Tso, Chang-An Yu, and Linda Yu

Biochimica et Biophysica Acta-Bioenergetics (2009) 1787, 913-919

Introduction

During electron transfer through the bc_1 complex, superoxide anion radicals ($O_2^{\cdot -}$) are generated (1-3). This is thought to result from the leakage of electrons from the low potential electron transfer chain, which react with molecular oxygen. The electron leakage site is speculated to be the ubisemiquinone radical of the Q_P site (4-6) or reduced heme b_L (7, 8). In fact, the electron leakage site (or superoxide generation site) in the bc_1 complex depends on which bifurcated quinol oxidation mechanism is functioning. At present, there are two popular potential mechanisms–the sequential and the concerted. Each has experimental support (9-13). In the sequential mechanism, ubiquinol gives its first electron to ISP to form ubisemiquinone at the Q_P site and then the electron from ubisemiquinone is transferred to heme b_L. In the concerted mechanism, the two electrons from ubiquinol are simultaneously transferred to ISP and heme b_L. If the sequential mechanism is functioning, the electron leakage sites are at the ubisemiquinone of the Q_P site and heme b_L. If the concerted mechanism is functioning, the only electron leakage site is at heme b_L. Regardless of which mechanism prevails, participation of the iron-

sulfur cluster is mandated. In other words, the electron that reacts with oxygen to generate superoxide originates from the second electron of ubiquinol. Since mutant bc_1 complexes lacking heme b_L or b_H (8) can generate superoxide to the same level as that of the antimycin inhibited wild-type complex, heme b_L is not a required component for superoxide generation. In the absence of heme b_L, molecular oxygen can act as a second electron acceptor during the bifurcated oxidation of QH_2 where the iron-sulfur cluster acts as the first electron acceptor at the hydrophobic Q_P pocket of the bc_1 complex. Since there is no semiquinone radical detected, the molecular oxygen and iron-sulfur cluster must receive electrons from QH_2 at about the same rate. The failure to detect superoxide formation in a mutant, which has the head domain of ISP fixed at the *b*-position with an elevated redox potential (6), is likely due to the lack of an oxidized form of the iron-sulfur cluster that is needed for the bifurcated oxidation of ubiquinol in order to produce superoxide. It is not due to the lack of mobility of the ISP head to reduce the accessibility of molecular oxygen.

Recently, the three-dimensional structure of the three-subunit core complex from *R. sphaeroides* has become available (14). However, the loss of subunit IV during crystallization decreases the usefulness of this bacterial structure in the study of interaction with subunit IV. In the proposed structural model of the *R. sphaeroides* bc_1 complex (15), subunit IV is located near cytochrome *b*, where the Q binding sites and heme b_L and b_H reside. This, together with the observation of superoxide production during bc_1 catalysis, encouraged us to suggest that subunit IV stabilizes cytochrome *b*, preventing electron leakage from the low potential electron transfer chain, thus increasing bc_1 activity. To test this hypothesis, the rates of cytochromes *b* and c_1 reduction, by

ubiquinol, and superoxide generation, by wild-type, three-subunit core and reconstituted complexes were determined and compared. Also, an inverse relationship between bc_1 activity and superoxide production was established.

Experimental Procedures

Materials – N-dodecyl-β-D-maltoside (DM) and N-octyl-β-D-glucoside were purchased from Anatrace. Ni-NTA resin was purchased from Qiagen. Glutathione-agarose gel, superoxide dismutase (SOD), xanthine oxidase, and Mn-containing superoxide dismutase (SOD) were purchased from Sigma. 2-Methyl-6-(4-methoxyphenyl)-3,7- dihydroimidazol[1,2-α]pyrazin-3-one, hydrocholoride (MCLA) was purchased from Molecular Probes. 2,3-Dimethoxy-5-methyl-6-10'bromo-decyl-1, 4-benzoquinol (Q_0C_{10} BrH_2) was synthesized in our laboratory as previously described (16).

Enzyme preparations and activity assay – The His_6-tagged, wild-type, and three-subunit core complexes were purified from chromatophores of BC17 carrying pRKD*fbc*FBC$_H$Q (17) and RSΔIV carrying pRKD*fbc*FBC$_H$ (15), respectively. Recombinant wild-type and mutant subunit IVs were prepared as described previously (18). Reconstituted bc_1 complexes were prepared by the addition of wild-type or mutant IVs to the three-subunit core complex at a 2:1 molar ratio and incubated for 1 hr at 0 ˚C (18). The concentrations of purified wild-type and mutant subunit IVs were determined by measuring the absorbance at 280 nm, using their respective millimolar extinction coefficients calculated according to the following equation (19):

$$\varepsilon^{280}{}_{mM} = 5.50\ (n_{Trp}) + 1.49\ (n_{Tyr}).$$

Where n = number of tryptophan or tyrosine residues present in wild-type or mutant subunit IVs. There are five tryptophan and three tyrosine residues in the wild-type IV.

The values of ε^{280}_{mM} used are 32 for wild-type and IV(R84E), 30.5 for IV(Y81A), and 29 for IV(81-84)A.

To assay electron transfer activity, purified cytochrome bc_1 complexes were diluted with 50 mM Tris-Cl, pH 8.0 containing 200 mM NaCl and 0.01% dodecyl maltoside to a final concentration of cytochrome *b* of 1 μM. Appropriate amounts of the diluted samples were added to 1 ml of assay mixture containing 100 mM Na^+/K^+ phosphate buffer, pH 7.4, 1 mM EDTA, 100 μM cytochrome *c* and 25 μM $Q_0C_{10}BrH_2$. Activity was determined by measuring the reduction of cytochrome *c* (the increase in absorbance at 550 nm) in a Shimadzu UV-2101PC, at 23 ˚C, using a millimolar extinction coefficient of 18.5 for calculation. Non-enzymatic reduction of cytochrome *c*, determined under the same conditions in the absence of enzyme, was subtracted from the assay.

Measurement of pre-steady state reduction rates of cytochromes b and c_1 – Measurements were performed in a stopped-flow apparatus, Applied Photophysics SX.18MV spectrometer (Leatherhead, England) with a photodiode array detector. The reaction was started by mixing equal volumes of solution A and solution B. Solution A contained 100 mM Na/K phosphate, pH 7.4, 1 mM KCN, 0.1% BSA, 0.01% DM and 12.0 μM of fully oxidized cytochrome bc_1 complex (based on cytochrome c_1) and solution B contained 5 mM NaH_2PO_4 1 mM KCN, 0.1%BSA, 0.01% DM and 240 μM $Q_0C_{10}BrH_2$, at 23 °C. The fully oxidized cytochrome bc_1 complexes were prepared by the treatment of isolated complexes with catalytic amounts of cytochrome *c* and cytochrome *c* oxidase, overnight, at 0 ˚C. The fully oxidized state was confirmed by absorption spectral analysis. To determine the reduction rates of cytochromes *b* and c_1, a

spectrum from 600 nm to 500 nm with a resolution of 2.17 nm was recorded every 2.08 msec. The dead time of the instrument was about 2 msec. Reductions of cytochromes *b* and c_1 were determined from the absorption changes at 560 nm-580 nm and 551 nm-539 nm, respectively. Time traces of the reaction were fitted with a first order rate equation to obtain the pseudo first order rate constants k_1 by Kaleidagraph.

To measure the effect of oxygen on the pre-steady state reduction of cytochrome *b*, oxygen was removed from solution A and solution B before mixing to start the reaction. Two test tubes containing solution A and solution B were placed in a sealed, three-arm bottle containing some water. Solution A was connected to syringe A by a flexible tubing with a T-joint through the first arm; solution B was connected to syringe B in a similar manner to solution A through the second arm; and the air space in the bottle was connected to a vacuum pump and argon gas through the third arm. The system was vacuumed and then followed by flushing with argon, repeatedly, for 1 min to replace oxygen in these two solutions with argon. After removing the oxygen, the solutions were forced into their respective syringes. The stopped-flow experiments were carried out in an Applied Photophysics stopped-flow reaction analyzer SX.18MV.

Measurement of superoxide anion – Superoxide anion generation was determined by measuring the chemiluminescence of MCLA- $O_2^{\cdot -}$ adduct (20-22) in an Applied Photophysics stopped-flow reaction analyzer SX.18MV by leaving the excitation light off and registering light emission, as previously reported (22). Reactions were carried out at 23 ˚C by mixing 1:1 solutions A and B. Solution A contains 100 mM Na^+/K^+ phosphate buffer, pH 7.4, 1 mM EDTA, 1 mM KCN, 0.1% BSA, 0.01% DM and 3 μM of wild-type or mutant bc_1 complex. Solution B was the same as A except that the bc_1 complex was

replaced with 50 μM $Q_0C_{10}BrH_2$ and 4 μM MCLA. The cytochrome bc_1 complexes used were in a completely oxidized form before mixing. $O_2^{\cdot -}$ generation is expressed in XO units. One XO unit is defined as chemiluminescence (maximum peak height of light intensity) generated by 1 unit of xanthine oxidase, which equals 2.0 V from an Applied Photophysics stopped-flow reaction analyzer SX.18MV.

Other biochemical methods – Cytochromes *b* (23) and c_1 contents (24) were determined as previously described.

Results and Discussions

Effect of subunit IV on the activation energy barrier of the cytochrome bc_1 complex – While the restoration of activity to the three-subunit core complex upon the addition of subunit IV is well established, the nature of this activation is not yet understood. It is important to know whether or not activation is due to a decrease of the activation energy barrier caused by interaction between the core complex and subunit IV. The activation energies of the wild-type and three-subunit core complexes were determined by Arrhenius plots of bc_1 activity in these two complexes (see Figure 14, below). An activation energy of 21.8 kJ/mol is obtained for the wild-type complex and 24.5 kJ/mol for the three-subunit core complex, at pH 7.4. Although the presence of subunit IV does somewhat decrease the activation energy of the bc_1 complex, it may not account for all of the activity enhancement; other factors may also be involved.

Effect of subunit IV on cytochrome b reduction by $Q_0C_{10}BrH_2$ – Figure 15 (page 65) shows time course traces of heme *b* reduction by $Q_0C_{10}BrH_2$ in wild-type (red) and

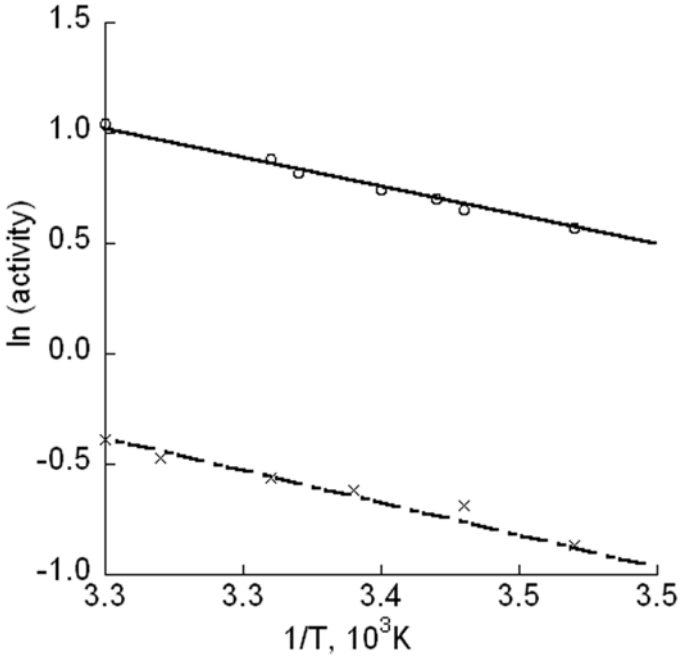

Figure 14. **Arrhenius plots for the electron transfer activities of wild-type and three-subunit core complexes.** The ubiquinol-cytochrome *c* activities in the wild-type (-o-) and three-subunit core complex (-x-) were assayed at every two degrees from 30 °C to 12 °C. The natural logarithms of the activities were plotted against the reciprocal of absolute temperature in an Arrhenius plot. The slopes of the Least Squares fitting straight lines were used to estimate their activation energies.

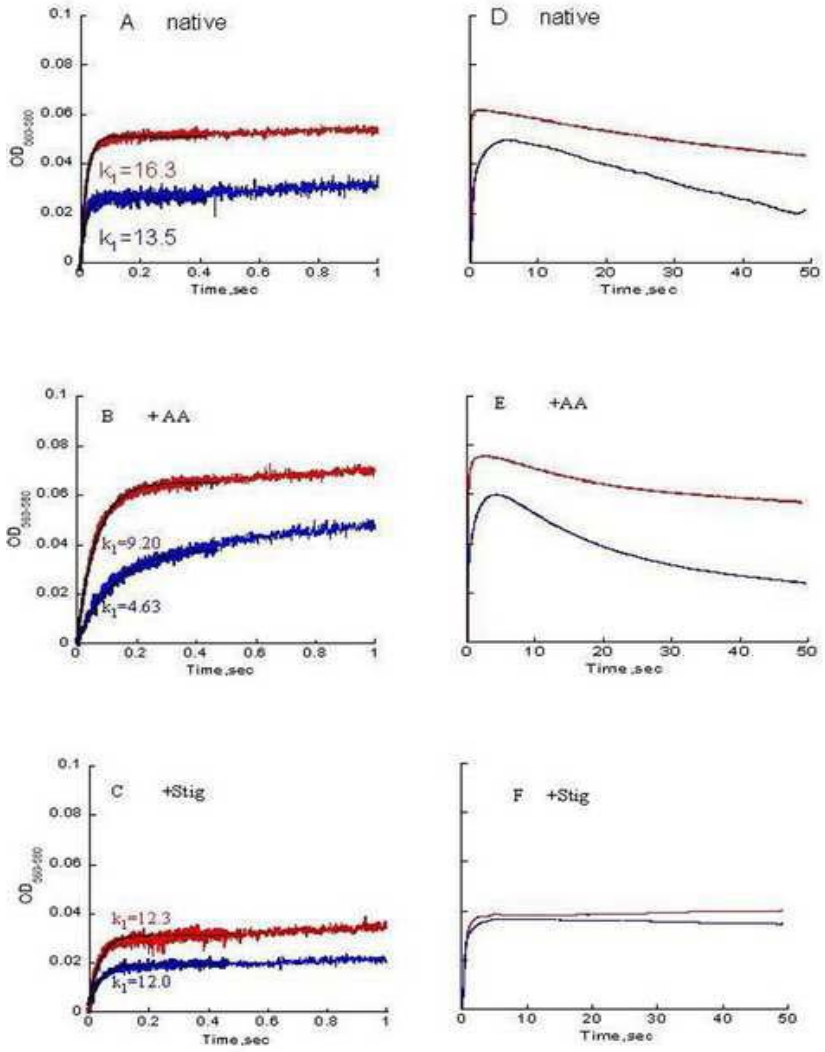

Figure 15. **Time courses of cytochrome *b* reduction by $Q_0C_{10}BrH_2$.** Wild-type (red) and three-subunit core (blue) complexes in the absence of inhibitors (panels A and D), and in the presence of antimycin A (panels B and E), or stigmatellin (panels C and F). Experimental conditions were as described in the "Experimental Procedure." The concentration of antimycin used was 30 µM and that of stigmatellin was 20 µM. The reduction of cytochrome *b* was followed by A_{560nm} - A_{580nm} . Solid lines represent fitted curves.

three-subunit core (blue) bc_1 complexes, in the absence (A & D) and presence of antimycin (B & E) or stigmatellin (C & F), at 1 and 50 sec time scales. Experiments were performed with a stopped-flow apparatus. $Q_0H_{10}BrH_2$ was added in 20-fold molar excess of the enzyme complex. Antimycin A is a Q_N site inhibitor which blocks electron transfer from heme b_H to ubiquinone. Stigmatellin is a Q_P site inhibitor whose binding to cytochrome *b* fixes the ISP head at the *b*-position. The final concentration of antimycin A was 30 μM and of stigmatellin was 20 μM.

In the absence of an inhibitor (see Figure 15A, above), the reduction kinetics of heme *b* in the wild-type and three-subunit core complexes are similar. They are both biphasic: a fast reduction phase followed by a slow reduction phase. The rate constants for the fast reduction phase of heme *b* in the wild-type and three-subunit core complexes are 16.3 s^{-1} and 13.5 s^{-1}, respectively. The extent of heme *b* reduction is much less in the three-subunit complex (0.027 O.D. unit) than in the wild-type complex (0.055 O.D. unit). The less than 20% decrease in the rate of heme *b* reduction in the three-subunit core complex does not account for the 50% decrease in the extent of heme *b* reduction. These results seem to suggest that, in the absence of subunit IV, some electrons may deviate from their normal pathway before they reach heme b_H during bc_1 *catalysis.* However, it is difficult to assess the site of electron leakage during bc_1 catalysis by comparing reduction kinetics of hemes *b* in these two complexes because heme b_H reduction by quinol in the bc_1 complex, according to the Q-cycle mechanism, is affected by (i) the forward reduction through the Q_P site to heme b_L and then to b_H; (ii) the reoxidation of reduced heme b_H by ubiquinone; and (iii) the "back door" reduction through the Q_N site.

Therefore, the reduction kinetic of heme *b* was examined with the aid of Q_N and Q_P site inhibitors.

The addition of antimycin A (see Figure 15B, page 65) increases the extent and decreases the rate of heme *b* reduction in the wild-type and three-subunit core complexes. However, the degree of effect varies in these two complexes. In the wild-type complex, the extent of heme *b* reduction increases by 27% (from 0.055 O.D. unit to 0.070 O.D. unit) while the reduction rate constant decreases by 44% (from 16.3 s^{-1} to 9.1 s^{-1}). In the three-subunit core complex, the extent of heme *b* reduction increases by 50% (from 0.030 to 0.045) and the reduction rate decreases by 67% (from 13.5 s^{-1} to 4.4 s^{-1}). Antimycin A blocks electron transfer from reduced heme b_H to ubiquinone and prevents reduction of heme b_H by $Q_0C_{10}BrH_2$ through the Q_N site. Thus, the rate and extent of heme *b* reduction by $Q_0C_{10}BrH_2$ in the presence of antimycin A is through the Q_P site via heme b_L. In the presence of antimycin A, the extent of heme *b* reduction in the three-subunit core complex (0.045 O.D. unit) is about 36% less than that in the wild-type complex (0.070 O.D. unit). This result further suggests that the absence of subunit IV facilitates electron leakage from the low potential electron transfer chain, reduced heme b_L or ubisemiquinone at the Q_P site, during bc_1 catalysis. When the wild type, three-subunit core, and reconstituted complexes were assayed for ubiquinol-cytochrome *c* reductase activity, about 9.5%, 13.1% , and 9.8% of their respective activities are insensitive to antimycin A. The increase in antimycin A-insensitive activity in the three-subunit core complex is in line with the suggestion of more electron leakage in this complex, because the portion of cytochrome *c* reduced by superoxide produced from the electrons linked

from the bc_1 complex at the Q_P site during catalysis is expected to be insensitive to antimycin A.

To further confirm this suggestion, the time course traces of heme *b* reductions in the wild-type and three-subunit core complexes, by Q_0C_{10} BrH_2, were extended to 50 sec (see Figure 15D and 15E, page 65). If this suggestion is correct, the extent of heme *b* reduction in the core complex should never reach the same level as that in the wild-type complex. This is indeed the case. In fact, the heme *b* reduction by quinol in both complexes, in the absence and presence of antimycin A, is biphasic: a fast reduction phase followed by a slow re-oxidation phase. This re-oxidation phase is not due to substrate limitation or to electron transfer from reduced heme b_H to ubiquionone because the concentration of $Q_0C_{10}BrH_2$ is 20 times that of cytochrome *b* and the system contains antimycin A (Figure 15E, page 65). The rate of re-oxidation in the three-subunit core complex is faster than that in the wild-type complex. This re-oxidation may result from electron leakage from the low potential electron transfer chain. Possibly the difference in the extent of heme *b* reduction in the wild-type and three-subunit core complexes results from the difference in the rate of electron leakage in these two complexes.

If the differences in the extents of heme *b* reduction and in the re-oxidation kinetics on the extended (50 sec) timescale originate from the leaks to oxygen, one would expect to see the diminishing of these differences (partly or completely) upon removal of oxygen. This is indeed the case. When reduction of cytochrome *b* in the wild-type and three-subunit core complexes, by $Q_0C_{10}BrH_2$, was determined under anaerobic conditions, the difference in the maximum extent of heme *b* reduction between these two complexes is 0.012 O.D. unit, a decrease of 20% compared to that obtained under aerobic conditions

(0.015 O.D. unit). The re-oxidation phases observed during cytochrome *b* reduction in the wild-type and three-subunit core complexes are completely diminished.

Addition of stigmatellin (Figure 15C, page 65) decreases the extent and rate of heme *b* reduction in the wild-type and three-subunit core complexes. The effects are similar in both complexes. In the presence of stigmatellin, heme *b* reduction in the three-subunit core complex (0.02 O.D. unit) is about 43% less than that in the wild-type complex (0.035 O.D. unit). Reduction rate constants are 12.3 s^{-1} and 12.0 s^{-1}, respectively. These results are as expected, since heme *b* reductions by $Q_0C_{10}BrH_2$, in the presence of stigmatellin, are through the Q_N site. No re-oxidation phase appears in the 50 sec time trace, indicating that there was no electron leakage in this electron transfer pathway.

To be sure that these observed differences in heme *b* reduction between the wild-type and three-subunit core complexes are indeed due to the lack of subunit IV, time course tracing of heme *b* reduction by $Q_0C_{10}BrH_2$ in the reconstituted complex formed from recombinant wild-type IV and the three-subunit core complex were determined. The rate and extent of heme *b* reduction in the reconstituted complex are the same as in the wild-type complex (data not shown), confirming that subunit IV decreases electron leakage during bc_1 catalysis.

Effect of subunit IV on the reduction of cytochrome c_1 in the bc_1 complexes – Figure 16 (below) shows time traces of cytochrome c_1 reduction in the wild-type (red) and three-subunit core (blue) complexes in the absence (A & D) and presence of antimycin A (B & E) or stigmatellin (C & F) in 1 sec and 50 sec time ranges. The heme c_1 reductions, in the absence of an inhibitor, by $Q_0C_{10}BrH_2$ in the wild-type and three-subunit core complexes are biphasic: a fast reduction phase followed by a slow reduction

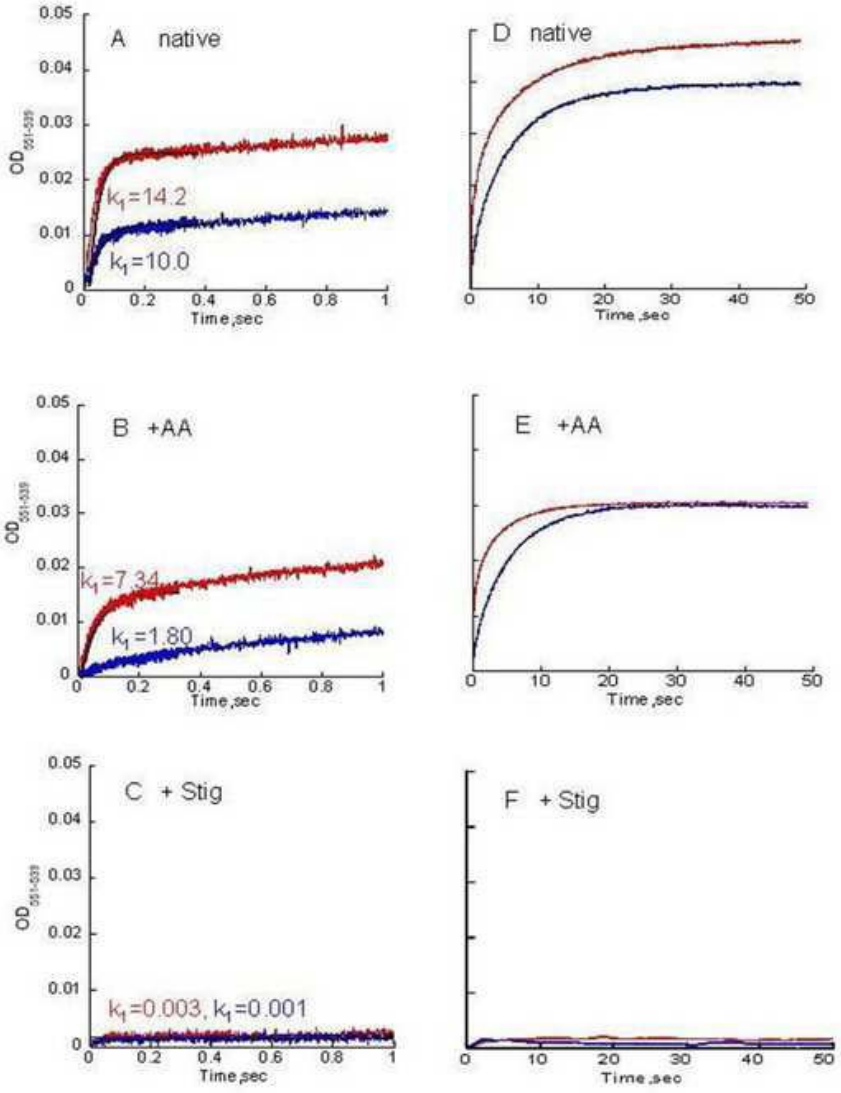

Figure 16. **Time courses of cytochrome c_1 reduction by $Q_0C_{10}BrH_2$.** Wild-type (red) and three-subunit core (blue) complexes in the absence of inhibitors (panel A and D) and in the presence of antimycin A (panels B and E) or stigmatellin (panels C and F). Experimental conditions were as described in Figure 15, except the reduction of heme c_1 was followed by $A_{551nm} - A_{539nm}$. Solid lines represent fitted curves.

phase (see Figure 16 A & B). The pseudo first order rate constants for the fast reduction phase are 14.2 s^{-1} and 10.0 s^{-1} for the wild-type and core complexes, respectively.

The addition of antimycin A decreases the rate of heme c_1 reduction by 49% (from 14.2 to 7.3 s^{-1}) in the wild-type complex and by 82% (from 10.0 to 1.8 s^{-1}) in the three-subunit core complex. These results are consistent with the previous report (8, 25) that antimycin A has a significant effect on the reduction rate of heme c_1 in cytochrome bc_1 complexes. This inhibitor effect has been attributed to the long range effect of antimycin on the Q_P site when binding to the Q_N site. Subunit IV has little effect on the Q_P site.

Although the reduction rate constants for heme c_1, upon addition of antimycin A, decrease drastically in both complexes, a maximum reduction of O.D. value of 0.03 is reached in both complexes (see Figure 16E, above). These results are consistent with the previous report (8, 25) that antimycin A has a significant effect on the reduction rate of heme c_1 in cytochrome bc_1 complexes. This inhibitor effect has been attributed to the long range effect of antimycin on the Q_P site when binding to the Q_N site (8, 25). Subunit IV has little effect on the Q_P site.

Since it is known that superoxide can reduce cytochrome *c*, it seems possible that part of this c_1 reduction results from heme c_1 being reduced by superoxide. To test this possibility, the extents of heme c_1 reduction in antimycin-treated intact, three-subunit core, and reconstituted wild-type complexes were measured in the presence of SOD. The extents of heme c_1 reduction in these three antimycin-treated complexes decrease in the presence of SOD. It is as expected that the extent of decrease (compared to that in the absence of SOD) is larger in the three-subunit core complex than the wild-type and

reconstituted wild-type complexes. These results are in line with the data obtained in the next section showing that the three-subunit core complex has higher superoxide generating activity than that of the wild-type or reconstituted wild-type complex.

Addition of stigmatellin to these two complexes abolishes heme c_1 reduction (see Figure 16F, page 70). These results confirm that the Q_P site in the three-subunit core complex is functional.

Effect of subunit IV on superoxide production by the cytochrome bc_1 complex – What is the fate of the leaked electron from the low potential electron transfer chain? One of the pathways is a reaction with molecular oxygen to form superoxide anion. If this is the correct pathway, one should see more superoxide production by the three-subunit core complex than the wild-type complex because more electrons leak from the former.

Production of superoxide by the cytochrome bc_1 complex can be determined by measuring the decrease in the rate of cytochrome *c* reduction in the presence of SOD under conditions of continuous turnover of the bc_1 complex. The small rate of cytochrome *c* reduction, compared with the normal rate of cytochrome *c* reduction, compromises the accuracy of this method. The MCLA-$O_2^{\cdot -}$ chemiluminescence method, which has been wildly used to measure $O_2^{\cdot -}$ production, is more sensitive than the cytochrome *c* method (20). However, use of the MCLA-$O_2^{\cdot -}$ chemiluminescence method to determine superoxide production during continuing turnover of the bc_1 complex (in the presence of ubiquinol and cytochrome *c*), encounters a high background rate of $O_2^{\cdot -}$ production resulting from the non-enzymatic oxidation of ubiquinol by cytochrome *c*, making it difficult to unambiguously compare $O_2^{\cdot -}$ production by various subunit IV mutant complexes. This difficulty has been overcome by measuring the

chemiluminescence of the MCLA-$O_2^{\cdot -}$ adduct during a single turnover of bc_1 complex using the Applied Photophysics stopped-flow reaction analyzer SX.18 MV by leaving the excitation light source off and registering light emission (22). Because the system contains no cytochrome *c*, chemiluminescence of MCLA-$O_2^{\cdot -}$ resulting from non-enzymatic oxidation of ubiquinol by cytochrome *c* is eliminated, enabling us to accurately evaluate changes in the rate of superoxide anion generation by various bc_1 complexes.

Figure 17, below, shows the tracings of $O_2^{\cdot -}$ generation by wild-type complex (curve 2), three-subunit core complex (curve 4), and reconstituted complex (curve 3). MCLA-$O_2^{\cdot -}$ chemiluminescence induced by bc_1 complex reaches peak intensity after about 0.06 s at room temperature, and then decays. Maximum peak height (0.158 V) induced by the three-subunit core complex (see curve 4) is about 4 times that of the wild-type complex (0.038 V) (see curve 2). It should be noted that maximum peak height was bc_1 complex concentration dependent. The addition of subunit IV to the core complex decreases $O_2^{\cdot -}$ production to about the same level as that of wild-type complex (see curve 3). No luminescence was detected when the bc_1 complex was omitted from the enzyme-containing solution or when $Q_0C_{10}BrH_2$ was omitted from the substrate-containing solution (curve 5). The addition of 300 units/ml superoxide dismutase to either the substrate or enzyme solution completely abolishes luminescence (curve 5), indicating that $O_2^{\cdot -}$ is responsible for the luminescence observed. These results clearly indicate that the presence of subunit IV decreases superoxide anion production by the bc_1 complex.

The decrease in superoxide production by the wild-type or reconstituted wild-type complexes may result from the slowed rate of superoxide releasing from its generating

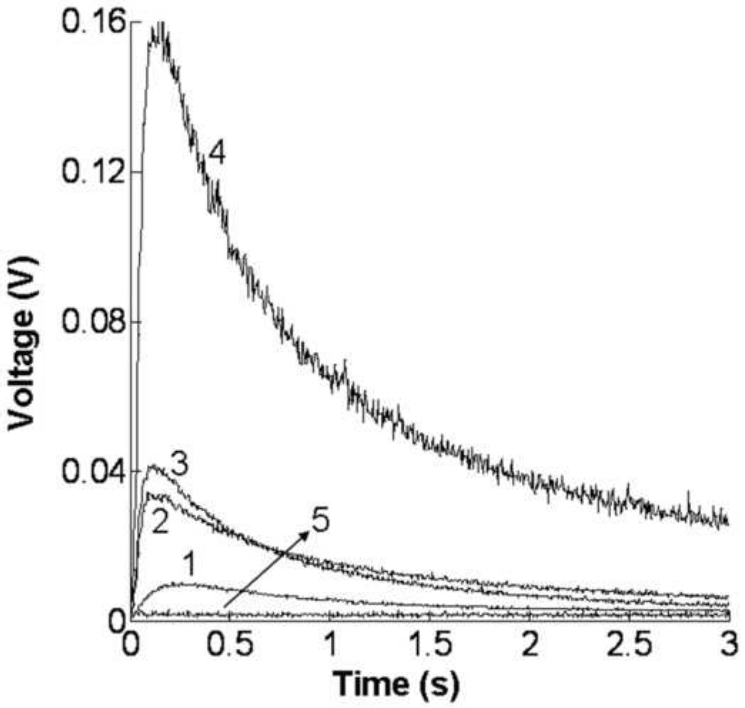

Figure 17. **Time traces of superoxide generation.** The superoxide generation reactions were carried out at 23 ºC in the Applied Photophysics stopped-flow reaction analyzer SX 18MV by mixing 1:1 solutions of A and B containing enzyme complexes and substrate as detailed in "Experimental Procedure." Curves 2 to 4 represent wild-type complex, the complex reconstituted from the core complex and recombinant wild-type IV, and the three-subunit core complex, respectively. Curve 1 shows superoxide generation by the beef heart bc_1 complex under the same conditions. Curve 5 is for control experiments when no bc_1 complexes or $Q_0C_{10}BrH_2$ was present in the system. A similar curve was obtained when 300 unit/ml Mn-SOD was added to the complete system.

site, the hydrophobic Q_P pocket, to the aqueous phase to react with MCLA. The Q_P pocket is more insulated in the wild type complex than that in the core complex, because subunit IV provides an additional physical barrier. This additional barrier may come from subunit IV itself or a minor structural change around the Q_P site of the cytochrome *b* protein induced by the presence of subunit IV. Therefore, the release of superoxide from the Q_P pocket of the wild-type complex would be slower than that of the core complex. One can imagine that in the hydrophobic Q_P pocket the reduced heme b_L and superoxide are in equilibrium. If the release of superoxide from the pocket proceeds with a slower rate, a higher heme b_L reduction will result, although the physical relationship between subunit IV and heme b_L is not yet established, due to the unavailability of the 3-D structure of a four-subunit complex. The closed relationship between the cytochrome *b* subunit and the subunit IV is, however, confirmed by the recovery of both subunits in the same fraction during subfractionation of the cytochrome bc_1 complex.

The relationship between electron transfer and superoxide anion generation in the cytochrome bc_1 complex – If our suggestion that the presence of subunit IV decreases superoxide production, thus increasing electron transfer activity in the three-subunit core complex, is correct, one should see an inverse relationship between electron transfer activity and superoxide production activity in bc_1 complexes having various degrees of functionally active subunit IV. Functional activity of subunit IV refers to its ability to interact with the three-subunit core complex to restore bc_1 activity. This activity is also called reconstitutive activity. The availability of recombinant mutant subunit IVs with varying reconstitutive activity in our laboratory enables us to prepare bc_1 complexes with varying electron transfer activities. Table 6, below, summarizes electron transfer and

Table 6. **Summary of the electron transfer and superoxide generating activities by various bc_1 complex preparations.**

Preparations	Electron Transfer μmol *c* /min/nmol *b*	Superoxide Production XO unit/nmol *b*	
		-AA	+AA
Wild type	2.42±0.03	0.07±0.01	0.23±0.02
Core complex	0.63±0.01	0.25±0.02	0.42±0.03
[Core complex + wild type IV]	2.32±0.03	0.07±0.01	0.23 ±0.02
[Core complex + IV(Y81A)]	2.03±0.02	0.09±0.01	0.27 ±0.03
[Core complex + IV (R84E)]	1.41±0.02	0.16±0.02	0.34 ±0.03
[Core complex + IV(81-84)A	0.92±0.01	0.21±0.02	0.38 ±0.03

The data represented were mean values ± standard deviations from three experiments.

superoxide anion production activities in various complexes in the presence and absence of antimycin A. The electron transfer activity, expressed as μmol cytochrome *c* reduced per min per nmol *b*, for the three-subunit core complex and reconstituted complexes formed from the core complexes and recombinant wild-type and mutant IVs, Y81A, IV(R84E), IV(81-84)A , are 0.6, 2.3, 2.0, 1.4, and 0.9, respectively. The $O_2^{\cdot -}$ production by these five complexes, expressed as XO unit per nmol *b*, are 0.25, 0.067, 0.092, 0.155, and 0.206, respectively (Table 6, above). These results indicate that the superoxide production by the bc_1 complex is inversely proportional to its electron transfer activity. In other words, the reconstituted complex, formed from the three-subunit core complex and subunit IV with higher reconstitutive activity, has higher electron transfer activity but lower superoxide generation activity. All these results support the idea that subunit IV decreases electron leakage, thus increasing electron transfer activity of the bc_1 complex. They also explain the observation that more complicated bc_1 complexes, such as bovine heart bc_1 complex, which have more supernumerary subunits, are more stable, have higher electron transfer activity, and generate much less superoxide anion during normal electron transfer (see Figure 17, curve 1, page 74).

Summary

There are three observations from this study. (1) The extent of cytochrome *b* reduction in the three-subunit core complex, by ubiquinol, in the presence of antimycin A, never reaches the same level as that in the wild-type complex; (2) the core complex produces 4 times as much superoxide anion as does the wild-type complex; and (3) when the core complex is reconstituted with subunit IVs having varying reconstitutive activities,

the activity increase in reconstituted complexes correlates with superoxide production decrease and extent of cytochrome *b* reduction increase. These observations indicate that the activity increase upon the addition of subunit IV to the three-subunit core complex, may result from subunit IV preventing electron leakage, from the low potential electron transfer chain, and reaction with molecular oxygen, producing superoxide anion.

References

1. Zhang, L., Yu, L., Yu, C. A. (1998) *J. Biol. Chem.* **273**, 33972-33976.
2. Muller, F., Crofts, A. R., Kramer, D. M. (2002) *Biochemistry* **41**, 7866–7874.
3. Sun, J., Trumpower, B. L.(2003) *Arch. Biochem. Biophys.* **419**, 198-206.
4. Muller, F., Roberts, A. G., Bowman, M. K., Kramer, D. M. (2003) *Biochemistry* **42**, 6493-6499.
5. Dröse, S., Brandt, U. (2008) *J. Biol. Chem.* **283**, 21649-21654.
6. Borek, A., Sarewicz, M., Osyczka, A. (2008) *Biochemistry* **47**, 12365-12370.
7. Nohl, H., Jordan, W. (1986) *Biochem. Bioph. Res. Commun.* **138**, 533-539.
8. Yang, S., Ma, H-W, Yu, L., Yu, C. A. (2008) *J. Bio. Chem*. **283**, 28767-28776
9. Cape, J. L., Bowman, M. K., Kramer, D. M. (2007) *Proc. Natl. Aca. Sci.* **104**, 7887-7892.
10. Zhu, J., Egawa, T., Yeh, S. R., Yu, L., Yu, C. A. (2007) *Proc. Natl. Aca. Sci.* **104**, 4864-4869.
11. Nikiforov, M., Anderson, J. L., Sweeny, E. *etc.* (2008) the biophysical society 52nd annual meeting abstract.
12. Osyczka, A., Moser, C. C., Daldal., F., Dutton, P. L. (2004) *Nature* **427**, 607-612.
13. Zhang, H., Osyczka, A., Dutton, P. L., Moser, C. C. (2007) *Biochim. Biophys. Acta* **1767**, 883-887.
14. Esser, L., Elberry, M., Zhou, F., Yu, C. A., Yu, L., Xia, D. (2008) *J. Biol. Chem.* **283**, 2846-2857.
15. Tso, S. C., Shenoy, S. K., Quinn, B. N., Yu, L. (2000) *J. Biol. Chem.* **275**, 15287-15294.

16. Yu, C. A., Yu, L. (1982) *Biochemistry* **21**, 4096-4101.

17. Tian, H., Yu, L., Mather, M. W., and Yu, C. A.(1998) *J. Biol. Chem.* **273** , 27953-27959.

18. Tso, S. C., Yin, Y., Yu, C. A., Yu, L. (2006) *Biochim. Biophys. Acta.* **1757**, 1561-1567.

19. Pace, C. N., Vajdos, F., Fee, L., Grimsley, G., Gray, T. (1995) *Protein Sci.* **4**, 2411-2423.

20. Nakano, M. (1990) *Methods Enzymol.* **186**, 585-591.

21. Denicola, A., Souza, J. M., Gatti, R. M., Augusto, O., Radi, R.(1995) *Free Radic. Biol. Med.* **19**, 11–19.

22. Gong, X., Yu, L., Xia, D., Yu, C. A. (2005) *J. Biol. Chem.* **280**, 9251-9257.

23. Berden, J. A., Slater, E. C. (1970) *Biochim. Biophys. Acta*. **216**, 237-249.

24. Yu, L., Doug, J. H., Yu, C. A. (1986) *Biochim. Biophys. Acta*. **852**, 203-211.

25. Snyder, C. H., Gutierrez-Cirlos, E. B., Trumpower, B. L. (2000) *J. Biol. Chem.* **275**, 13535-13541.

CHAPTER IV

REACTION MECHANISM OF SUPEROXIDE GENERATION DURING UBIQUINOL OXIDATION BY THE CYTOCHROME *bc*$_1$ COMPLEX

Introduction

It has long been recognized that during mitochondrial respiration there is a continuous release of electrons from the electron transfer chain to molecular oxygen (O_2) to form a superoxide anion ($O_2\cdot^-$) (1-3). The generated $O_2\cdot^-$ is subsequently dismutated to H_2O_2 spontaneously or by the action of superoxide dismutases (SOD) (4). Isolated mitochondria in state 4 generate 0.6-1.0 nmol of H_2O_2/min/mg protein, accounting for about 2% of O_2 uptake under physiological conditions (5). Production of $O_2\cdot^-$ during mitochondrial respiration is closely related to mitochondrial coupling efficiency. More $O_2\cdot^-$ is produced when the membrane potential of mitochondria is high (6).

Two segments of the respiratory chain have been demonstrated to be responsible for the generation of $O_2^{\cdot-}$ from dioxygen. One is located at the NADH-Q oxidoreductase (complex I) and the other is at the cytochrome *bc*$_1$ complex (ubiquinol-cytochrome *c* oxidoreductase). Production of $O_2\cdot^-$ by complex I is either via auto-oxidation of the

flavine radical in NADH dehydrogenase (7) or via a bound ubiquinone radical (8) or the center N-2 (9) of the complex. It was recently suggested (10) that the reversed electron transport through complex I produced more $O_2\cdot^-$ than the forward transport. Two redox components of the bc_1 complex, ubisemiquinone at the Q_P site (11) and the reduced cytochrome b_{566} (12,13), have been implicated as electron donors for molecular oxygen to generate $O_2\cdot^-$. The production of $O_2\cdot^-$ by the bc_1 complex is greatly enhanced when the complex is inhibited by antimycin (13-15).

In the past, most information concerning mitochondrial $O_2\cdot^-$ generation sites was obtained from studies using intact heart mitochondria with selected electron transfer inhibitors by measuring H_2O_2 concentration in the suspending medium (11, 12). More recently, studies of $O_2\cdot^-$ formation are carried out with purified electron transfer complexes, such as NADH-ubiquinone reductase (7, 8), succinate-cytochrome *c* reductase (13) or cytochrome bc_1 complex (15). Although results obtained with purified complex are less ambiguous than those obtained with mitochondria, the $O_2\cdot^-$ generating sites in NADH-Q oxidoreductase and bc_1 complex remain controversial. Evidence supporting the flavin (7) radical and the ubiquinone radical (8) as the electron donor for the $O_2\cdot^-$ generation in complex I are both available. Arguments favoring the reduced cytochrome b_L or ubisemiuquinone radical as the electron donors for molecular oxygen to generate $O2\cdot^-$ continue (16).

In continuing our study of the structural and functional relationship of the bc_1 complex, it is important to understand the reaction mechanism of superoxide generation in this complex. The fact that antimycin inhibits the electron transfer activity of the

cytochrome bc_1 complex and stimulates the $O_2\cdot^-$generating activity, together with the observation that both activities have a similar activation energy, led investigators to believe that both activities share, at least, a common intermediate (17). According to the Q-cycle mechanism, during the catalytic reaction of the cytochrome bc_1 complex, QH_2 undergoes bifurcated oxidation by transferring its two electrons, sequentially or simultaneously (concerted), to the iron-sulfur cluster (ISC) of the iron-sulfur protein (ISP) subunit and heme b_L of the cytochrome *b* subunit. In the sequential mechanism, ubiquinol transfers its first electron to the ISC to become low potential ubisemiquinone that contains a free electron and reduces cytochrome b_L instantly. In the concerted mechanism, no semiubiquinone is formed and two electrons of QH_2 are transferred simultaneously to ISC and heme b_L. This bifurcated electron transfer reaction provides a basis for the high efficiency of the bc_1 complex and is done inside the cyt. *b* subunit buried in the membrane bilayer. It is, thus, expected that any compromise in the structural integrity of cytochrome *b* should lead to a decrease in the electron transfer efficiency and to an increase in the production of superoxide. The observation that mutants lacking heme b_L or heme b_H, respectively, shows little electron transfer activity but high superoxide generating activity is consistent with the idea that the structural integrity of cytochrome *b* is required for normal electron transfer activity but not for superoxide generation.

Herein we report a systematic comparison of the electron transfer and $O_2\cdot^-$ generating activities in various cytochrome bc_1 complexes having varying numbers of supernumeral subunits or with different extents of heat inactivation, or protease K digestion to see whether or not the intact protein components of the complex are

required for $O_2\cdot^-$ generating activity. We also determined the effect of ubiquinol, phospholipid vesicles, detergent micelles, cytochrome *c*, and ferricyanide concentration on superoxide anion generation to establish that an electron donor – ubiquinol, a high potential electron acceptor ISC, cytochrome *c*, or ferricyanide – and a hydrophobic environment are responsible for $O_2\cdot^-$ production. Based on the results obtained, we formulated a working hypothesis for the reaction mechanism of superoxide production in the bc_1 complex.

Experimental Procedures

Materials – Cytochrome *c* (horse heart, type III) was purchased from Sigma. Proteinase K was purchased from Invitrogen. *N*-Dodecyl-D-Maltopyranoside (LM) and *N*-octyl- D-Gluocopyranoside (OG) were obtained from Anatrace. Nickel nitrilotriacetic acid gel and a Qiaprep spin Miniprep kit were obtained from Qiagen. 2-Methyl-6- (4-methoxyphenyl)-3, 7-dihydroimidazol[1, 2-α] pyrazin-3-one, hydrochloride (MCLA) was obtained from Molecular Probes, Inc. 2,3-Dimethoxy-5-methyl -6-(10-bromodecyl)-1,4-benzoquinol($Q_0C_{10}BrH_2$) was prepared as previously reported (18). All other chemicals were of the highest purity commercially available.

Enzyme preparations and activity assays – Chromatophores, intracytoplasmic membrane (ICM), and the His_6-tagged cytochrome bc_1 complexes, wild-type (19) and mutants (20, 21), were prepared as previously reported. Bovine heart mitochondrial cytochrome bc_1 complex was prepared according to the method developed in our lab (22, 23).

To assay the cytochrome bc_1 complex activity, chromatophores or purified cytochrome bc_1 complexes were diluted with 50 mM Tris-Cl, pH 8.0, containing 200 mM NaCl and 0.01% DM to a final concentration of cytochrome c_1 of 1 µM. Appropriate amounts of the diluted samples were added to 1 ml of assay mixture containing 100 mM Na^+/K^+ phosphate buffer, pH 7.4, 300 µM of EDTA, 100 µM of cytochrome *c*, and 25 µM of $Q_0C_{10}BrH_2$. Activities were determined by measuring the reduction of cytochrome *c* (the increase of absorbance at 550 nm) in a Shimadzu UV 2101 PC spectrophotometer at 23 °C, using a millimolar extinction coefficient of 18.5 for the calculation. The non-enzymatic oxidation of $Q_0C_{10}BrH_2$, determined under the same conditions in the absence of the enzyme, was subtracted from the assay.

Digestion of the cytochrome bc_1 complex by proteinase K – A stock solution of proteinase K, 3%, was made in 10 mM Tris-HCl, pH 7.5, containing 20 mM of CaCl, and 50% of glycerol. Two µl of proteinase K solution was added into 200 µl of cytochrome bc_1 complex, 200 µM cyt. *b*, in 50 mM Tris-HCl, pH 8.0, containing 200 mM of NaCl and 0.01% of DM. The mixture was incubated at the room temperature. The electron transfer and $O_2^{\cdot -}$ generating activities were measured during the course of incubation until all the electron transfer activity was diminished. The digested bc_1 was then subjected to SDS-PAGE to confirm that all the subunits were digested.

Preparation of phospholipid vesicles – Phospholipid (PL) vesicles were prepared by the cholate-dialysis method (24). Azolectin was dissolved in chloroform and dried as a thin film against the tube by flushing with nitrogen gas while the tube is rotating. The phospholipid was then suspended in 50 mM K/Na phosphate buffer, pH 7.4, containing 1% of sodium cholate. The mixture was subjected to sonification intermittently for 10 min

until the solution become clear and then dialyzed against the same buffer overnight, with three changes of buffer.

Determination of superoxide production – $O_2\cdot^-$ production was determined by measuring the chemiluminescence of MCLA-$O^{\cdot-}$ adduct (25) in an Applied Photophysics stopped-flow reaction analyzer SX.18MV (Leatherhead, England) by leaving the excitation light off and registering light emission (26). Reactions were carried out at 23 °C by mixing 1:1 of solutions A and B. For the determination of $O_2\cdot^-$ productions by the native, heat-inactivated, or Proteinase K-digested cytochrome bc_1 complexes, Solution A contains 100 mM Na^+/K^+ phosphate buffer, pH 7.4, 1 mM EDTA, 1 mM KCN, 1 mM NaN_3, 0.1% bovine serum albumin, 0.01% LM, and 5.0 µM of cytochrome bc_1. Solution B contains 125 µM $Q_0C_{10}BrH_2$ and 4 µM MCLA in the same buffer. For the determination of $O_2\cdot^-$ productions in the presence of detergents, Solutions A contains 100 mM Na^+/K^+ phosphate buffer, pH 7.4, and 5.0 µM of cytochrome *c* and appropriate amount of detergent. Solution B contains 125 µM $Q_0C_{10}BrH_2$ and 4 µM MCLA in the same buffer. Once the reaction started, the produced fluorescence, in voltage, was consecutively monitored for 2 seconds.

Results and Discussion

The inverse relationship between superoxide generating and electron transfer activities in the cytochrome bc_1 complex – Table 7 (below) summarizes the electron transfer and $O_2\cdot^-$ generating activities in various bc_1 complex preparations. The bovine heart mitochondrial complex has eleven protein subunits. This complex has the highest electron transfer activity and lowest superoxide generating activity among the complexes

Table 7. **Comparison of the electron transfer and superoxide generating activities of various cytochrome bc_1 complexes.**

Preparation	Activity		
	Electron Transfer (μmoles *c* red/ min/nmoles c_1)	$O_2^{\cdot -}$ generating (munit XO / nmoles c_1)	
		-AA	+AA
Mitochondrial bc_1	43.0	14	18
Rs bc_1	3.5	91	300
ΔIV, Rs bc_1	0.8	325	546
Δb_L, Rs bc_1, H198N	0.4	510	510
Δb_H, Rs bc_1 H111N	0.3	500	510

tested. The *Rhodobacter spehaeroides* complex, which contains four protein subunit (three core subunits and one supernumerary subunit), has only about one tenth of the electron transfer activity of the bovine complex, but has about 7 times the $O_2 \cdot^-$ generating activity of the bovine enzyme. When the only supernumerary subunit (subunit IV) is deleted from the *Rhodobacter sphaeroides* wild-type complex, the resulting three-subunit core complex (RSΔIV) has only a fraction of the electron transfer activity of the wild-type complex, with about four times the $O_2 \cdot^-$generating activity of the wild-type complex. When the three-subunit core complex is reconstituted with subunit IV, the electron transfer activity increases and the $O_2 \cdot^-$ generating activity decreases to the same level as those in the wild-type, 4-subunit complex. These results suggest that the complexes with more supernumerary subunits have higher electron transfer activity but lower superoxide generating activity than the complexes with fewer supernumerary subunits.

The DSC studies indicate that the order of thermal stability among these complexes is: beef > wild-type *R. sphaeridies complex* = reconstituted complex> RSΔIV complex (data not shown). Therefore, the electron transfer activity of the bc_1 complex is in direct proportion to the structural integrity of the complex, whereas the superoxide generating activity has an inverse relationship with the structural integrity of the complex. In other words, the electron transfer activity is inversely proportional to the superoxide generating activity in the bc_1 complex.

The finding that the cytochrome bc_1 complex with less structural integrity has higher $O_2 \cdot^-$ generating activity encouraged us to speculate that $O_2 \cdot^-$ is generated inside the complex, perhaps in the hydrophobic environment of the Q_P pocket, and that the protein subunits, at least those surrounding the Q_P pocket, may play a role either in preventing

the release of $O_2\cdot^-$ from its production site to aqueous environments or in preventing O_2 from getting access to the hydrophobic pocket.

The superoxide generating activity in the heat inactivated cytochrome bc_1 complex – If the above speculation is correct, then one should see an increase in $O_2^{\cdot-}$ generation in the complex with denatured protein subunits. To test this speculation, the wild-type *R. sphaeroides* bc_1 complex was incubated at 37 ˚C to inactivate the complex, and the electron transfer and $O_2^{\cdot-}$ production activities were measured during the course of incubation (see Figure 18, below). As shown, the electron transfer activity decreases, whereas the $O_2\cdot^-$ generating activity increases, as the incubation time increases. Maximum $O_2^{\cdot-}$ generating activity is obtained when more than 90% of the electron transfer activity is abolished. This result indicates that the production of $O_2^{\cdot-}$ during quinol oxidation by cytochrome *c* does not require the presence of an intact bc_1 complex. The impairment of the structural integrity of the complex by the heat denaturation of the protein subunits leads to the increase in the accessibility of molecular oxygen to the hydrophobic environment of the Q_P pocket to generate $O_2^{\cdot-}$ and to facilitate the release of produced $O_2\cdot^-$ to the aqueous medium.

The notion that an intact protein subunit structure is not required for superoxide generating activity of the cytochrome bc_1 complex is further supported by the observation that mutants, H198N and H111N, which lack heme b_L and heme b_H**,** respectively, have very little electron transfer activity, but show $O_2\cdot^-$ generating activity equal to that of the antimycin-treated wild-type complex (Table 7, page 87). The loss of either heme *b*s would be expected to have a strong impact on the overall structural integrity of the bc_1 complex, leading to the distortions of the Q_P pocket environment and presumably

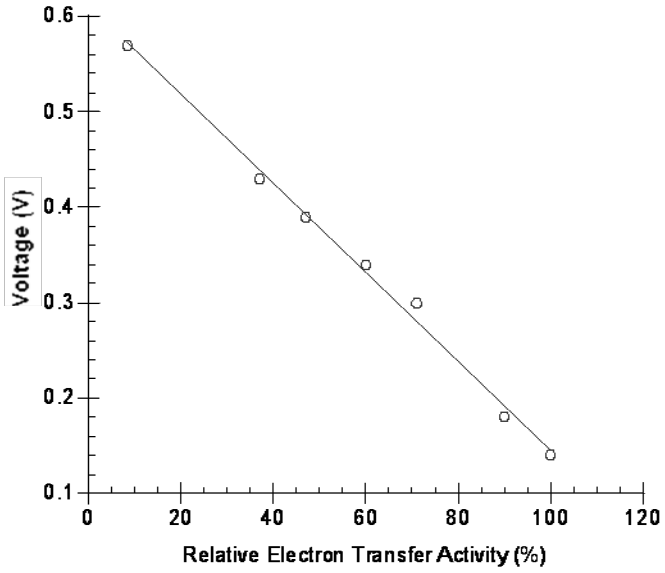

Figure 18. **The relationship between the electron transfer activity and superoxide generation during temperature inactivation of cytochrome *bc*$_1$ complex.** 200 µl of cytochrome *bc*$_1$ complex, 200 µM cyt. *b* in 50 mM Tris-Cl, pH 8.0, containing 200 mM NaCl and 0.01% LM, was incubated at 37 ˚C. Superoxide production (shown as voltage) and electron transfer activities (shown as relative electron transfer activity) were determined at various incubation times. Electron transfer activity and the superoxide production were measured as described in "Experimental Procedures." Solution A contains 100 mM Na^+/K^+ phosphate buffer, pH 7.4, 1 mM EDTA, 1 mM KCN, 1 mM NaN_3, 0.1% bovine serum albumin, 0.01% DM, and 5.0 µM of incubated cytochrome *bc*$_1$. Solution B was the same as A with *bc*$_1$ complex being replaced with 125 µM $Q_0C_{10}BrH_2$ and 4 µM MCLA.

increasing the accessibility of O_2 to the site. It is as expected that incubation of two mutant complexes at 37 ˚C to denature the protein subunits does not further increase the $O_2\cdot^-$ generating activity because the structural integrity of these two complexes has already been deteriorated by mutation.

The $O_2\cdot^-$ generating *activity in proteinase-K digested complex* – To further confirm that superoxide generating activity is independent of the presence of an intact protein structure, the bc_1 complex was subjected to protease K digestion and the electron transfer and superoxide generating activities were measured during the course of digestion. As shown in Figure 19, below, the electron transfer activity diminishes, whereas the $O_2\cdot^-$ generating activity increases, as the digestion time increases. Maximum superoxide generating activity is observed when electron transfer activity is completely abolished. SDS-PAGE analysis of the protease K-digested complex reveals no intact subunits of cytochromes *b*, c_1, or ISP (Figure 20, page 93). The largest peptide band presence in the digested complex has an apparent molecular weight of less than 7 kDa in SDS-PAGE. These results further support our suggestion that the intact protein components of the complex or the intact complex play no direct role in $O_2\cdot^-$ generation. Rather, a disrupted complex is a direct cause for $O_2\cdot^-$ production. The intact protein subunits or subunit structures serve as a barrier to prevent the molecular oxygen from gaining access to the hydrophobic environment of the Q_P pocket to form superoxide or to prevent the formed superoxide from releasing to the aqueous medium.

If this notion is correct, then what remaining elements in the proteinase K digested complex contributed to superoxide production from QH_2? A hydrophobic

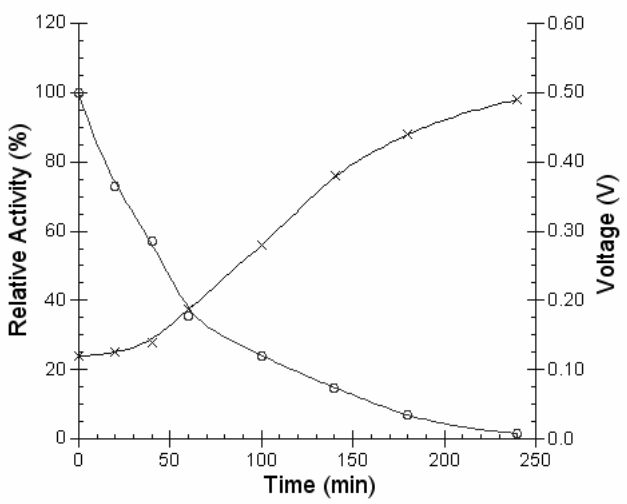

Figure 19. **Activity tracing of the electron transfer and $O_2 \cdot^-$ generation during the course of proteinase K digestion of the complex.** 200 µl of cytochrome bc_1 complex, 200 µM cyt. *b* in 50 mM Tris-Cl, pH 8.0, containing 200 mM NaCl and 0.01% LM, was incubated with 60 µg proteinase K at 37 ˚C. Superoxide production (-x-x-) and electron transfer (-o-o-) activities were determined at various incubation times as described in the legend of Figure 18.

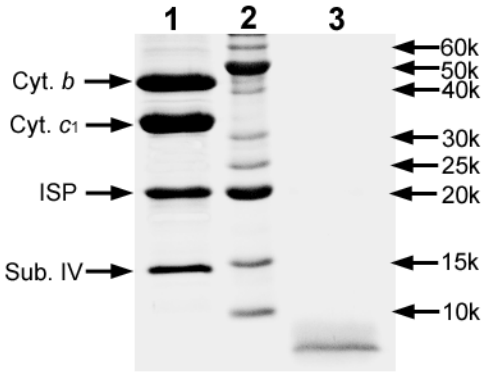

Figure 20. **Sodium dodeceyl sulfate gel electrophoresis of the cytochrome bc_1 complex and its proteinase K digested products.** Lane 1: intact wild type cytochrome bc_1; Lane 2: standard polypeptide; Lane 3: proteinase K-treated wild type. Aliquots of purified bc_1 complex samples were incubated with 1% SDS with 0.4% β-ME at 37 °C for 20 minutes. Digested samples containing around 200 pmoles of cytochrome c_1 were subjected to electrophoresis.

environment and a high potential electron acceptor ISC in the digested system could contribute to the superoxide formation in the presence of molecular oxygen. The presence of intact ISC in the proteinase K digested complex was confirmed by showing EPR signals of ISC in the digested complex. Thus, it is possible that ISC serves as a high potential electron acceptor and oxygen as another electron acceptor during bifurcated oxidation of QH_2 in a hydrophobic environment of the Q_P pocket to produce superoxide.

Generation of $O_2\cdot^-$ upon oxidation of ubiquinol by cytochrome c or ferricyanide in the presence of phospholipids vesicles – Although the addition of cytochrome *c* or ferricyanide to proteinase K-digested complex can increase its superoxide production, oxidation of ubiquinol by ferri-cytochrome *c* or ferricyanide in the aqueous solution at neutral pH is a very slow reaction and little $O_2\cdot^-$ formation is detected, suggesting that a hydrophobic environment provided by the digested complex is required for superoxide production. To confirm this suggestion, varying amounts of phospholipid vesicles were added to a system containing constant amounts of ubiquinol and cytochrome *c* and the superoxide anion production was measured. In the presence of phospholipid vesicles, the formation of $O_2\cdot^-$ is observed and the amount of $O_2\cdot^-$ generation is proportional to the amount of vesicles added (see Figure 21, below). This result clearly indicates that the formation of $O_2\cdot^-$ takes place in hydrophobic environments.

Detergents can facilitate superoxide production by QH_2 and cytochrome c – If the hydrophobic environment in the interior of phospholipids vesicles can facilitate $O_2\cdot^-$ generation, one would expect that a micellar solution of detergent should do the same. To test the effects of detergents on the $O_2\cdot^-$ production by QH_2 and cytochrome *c*, both non-

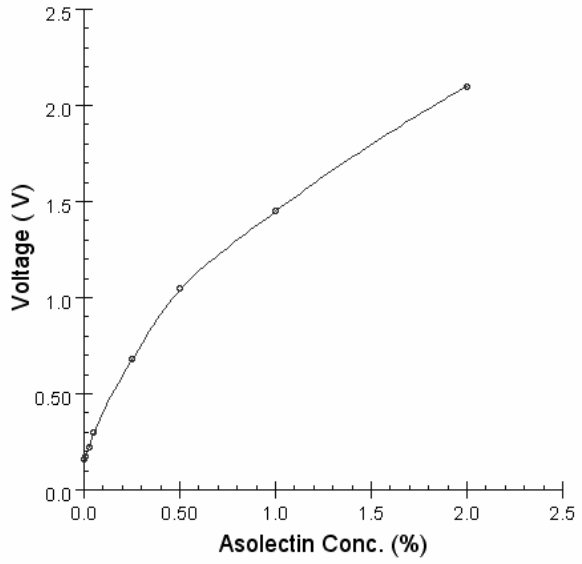

Figure 21. **Phopholipid vesicle concentration dependent superoxide formation under the constant amounts of cytochrome *c* and ubquinol.** The superoxide production was measured as described in "Experimental Procedures." Solution A contains 100 mM Na^+/K^+ phosphate buffer, pH 7.4, 5.0 µM of cytochrome *c*, and different concentrations of asolectin. Solution B contains 100 mM Na^+/K^+ phosphate buffer, pH 7.4, 125 µM of QH_2, and 4 µM of MCLA.

ionic detergents (OG and LM) and ionic detergents (sodium cholate and deoxycholate) were used to substitute phospholipids vesicles. Figure 22 ,below, shows the effect of detergent concentration on the superoxide production during quinol oxidation by cytochrome *c*. As expected, little $O_2^{\cdot -}$ generation is observed when the concentration of detergent used is below its critical micellar concentration (CMC) because no hydrophobic environment is available. When the concentration of detergent used is higher than its CMC, the $O_2^{\cdot -}$ production increases as the detergent micellar concentration in the system increases. The amount of $O_2^{\cdot -}$ production depends on the amount of QH_2, or high potential oxidant, available to the system. Interestingly, sodium cholate (SC) or deoxycholate (DOC) is a much more potent superoxide generator than either octyglucoside (OG) or dodecyl maltoside (LM). The CMCs for OG, LM, DOC, and SC are 25, 0.15, 1.33, and 3 mM (27), respectively, which do not appear to correlate with the observed abilities for their respective superoxide generations. Perhaps their superoxide generating abilities are related to their aggregation numbers. The aggregation number of a detergent represents an average micellar size. The aggregation numbers for SC, DOC, OG, and LM are 5, 55, 27, and 98, respectively. Except for OG, the aggregation numbers correlate better with their superoxide generating ability. These results suggest that the accessibility of a detergent to the hydrophobic interior is more important than the hydrophobicity of that detergent. Apparently, the lower aggregation number suggests a less well ordered micelle with a better accessibility to its hydrophobic core. The detergent with the higher aggregation number would indicate a well-ordered micelle with a hydrophobic interior that is difficult to gain access to. These results are consistent with

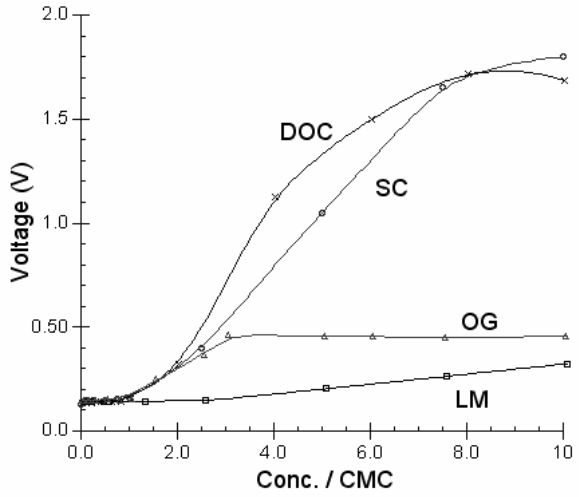

Figure 22. **Effect of detergents on the superoxide generation under the constant amounts of cytochrome *c* and ubiquinol.** The superoxide generation was measured as described in "Experimental Procedures." Solution A contains 100 mM Na^+/K^+ phosphate buffer, pH 7.4, 5.0 µM of cytochrome *c*, and different concentrations of detergents (LM, OG, SC and DOC). Solution B contains 100 mM Na^+/K^+ phosphate buffer, pH 7.4, 125 µM of QH_2, and 4 µM of MCLA.

the idea that the amount of accessible hydrophobic environment plays a key role in $O_2 \cdot^-$ generation on the oxidation of QH_2 by a high potential oxidant.

Superoxide anion generation is ubiquinol and oxidant concentration dependent – Generation of $O_2 \cdot^-$ requires an electron donor ubiquinol, and a high potential oxidant such as ISC, cytochrome *c*, or ferricyanide as an electron acceptor. To test the cytochrome *c* concentration dependency of $O_2 \cdot^-$ generation, various concentrations of cytochrome *c* were added to a reaction mixture containing 25 μM of QH_2 and 4 mM of sodium cholate (curve 1 in Figure 23, below). It is clear that the superoxide production is proportional to the concentration of cytochrome *c*. Curve 2 of Figure 23 shows the effect of ferricyanide concentration on the superoxide anion generation. Varying concentrations of ferricyanide were added to a reaction mixture containing 25 μM of QH_2, and 4 mM sodium cholate. Like cytochrome *c*, the superoxide production is proportional to the concentration of ferricyanide added.

The effect of QH_2 concentration on superoxide generation was also studied. Under a constant concentration of cytochrome *c* (2.5 μM) and sodium cholate (4 mM), superoxide production increases when QH_2 concentration increases, up to 30 μM (See Figure 24, page 100).

Reaction mechanism of $O_2 \cdot^-$ generation by the cytochrome bc_1 complex – Based on the results obtained that a superoxide anion is produced during QH_2 oxidation by cytochrome *c* or ferricyanide in the presence of phospholipid vesicles or a detergent micelle, and that the superoxide anion is produced by heat-inactivated or proteinase K digested complex, a reaction mechanism for superoxide production in the bc_1 complex is proposed. In this proposed mechanism, four elements are directly involved in superoxide

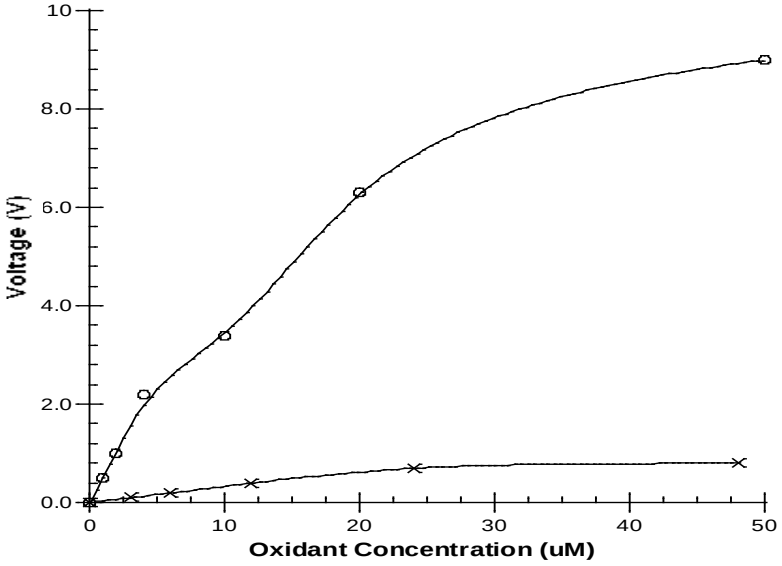

Figure 23. **High potential oxidant (cytochrome *c* or ferricyanide) concentration dependent superoxide generation under a constant amount of ubiquinol.** The superoxide production was measured as described in "Experimental Procedures." The curve with o (-o-o-) represents ferricyanide, and the curve with x (-x-x-) represents cytochrome *c*. Solution A contains 100 mM Na^+/K^+ phosphate buffer, pH 7.4, 4 mM sodium cholate, and a different concentration of cytochrome *c* or fericyanide. Solution B contains 100 mM Na^+/K^+ phosphate buffer, pH 7.4, 4 mM sodium cholate, 125 μM of QH_2, and 4 μM of MCLA.

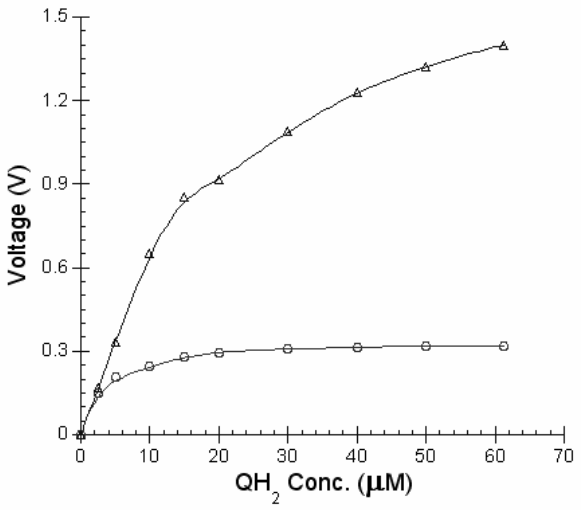

Figure 24. **Quinol concentration dependent superoxide productions under a constant amount of sodium cholate.** The superoxide production was measured as described in "Experimental Procedures." Solution A contains 100 mM Na^+/K^+ phosphate buffer, pH 7.4, 16 mM of sodium cholate, and 5 (-o-o-) or 50 (-Δ-Δ-) μM of cytochrome *c*. Solution B contains 100 mM Na^+/K^+ phosphate buffer, pH 7.4, 4 μM of MCLA, and different concentrations of QH_2.

generation. These are a hydrophobic environment, a high potential electron acceptor, a low potential electron acceptor, and an electron donor. The only protein subunit of the complex directly involved in the superoxide production is ISP or ISC bearing peptide, serving as the high potential electron acceptor.

The hydrophobic environment in the bc_1 complex is provided by the quinol oxidation pocket (the Q_P pocket) which is surrounded by residues from the cytochrome *b* subunit and a part of the iron-sulfur protein. Quinol undergoes bifurcated oxidation in this pocket by simultaneously transferring its two electrons to ISC and molecular oxygen to produce $O_2{\cdot}^-$. It is expected that the benzoquinol ring of QH_2 is located at the surface of the lipid bilayer or detergent micelles with its 1-hydroxy group extended into the water phase and the 4-hydroxy group together with its alky side chain located inside the bilayer or micelle (See Figure 25, page 102). When the ISC is used as an electron acceptor, a hydrogen is transferred from the 1-hydroxyl group to the e-N of the imidazole ring of histidine residue, which is a ligand of the ISC. At the same time, a hydrogen is transferred from the 4-hydroxy group to a molecule of oxygen to generate a protonated superoxide (HO_2) which then diffuses to the water phase to become a superoxide anion upon deprotonation.

The high potential electron acceptor ISC can be substituted with cytochrome *c* or ferricyanide. In this case, the 1-hydroxy group of ubiquinone is deprotonated and releases a proton to the water phase before the electron is transferred to ferricyanide or cytochrome *c*. At the same time, the 4-hydroxy group transfers its hydrogen atom to a molecular oxygen.

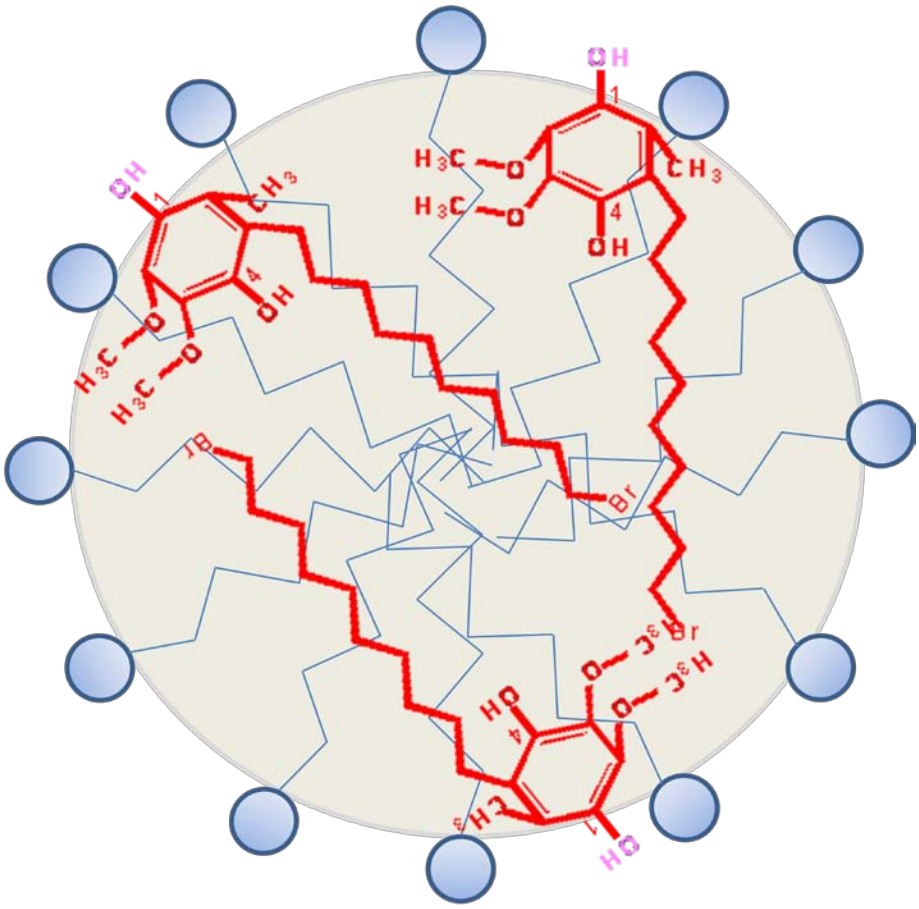

Figure 25. **The proposed location of $Q_0C_{10}BrH_2$ in the detergent micelle enviroment.**

According to this proposed $O_2\cdot^-$ generation mechanism, the generation of only a fraction of $O_2\cdot^-$ during quinol oxidation by cytochrome *c* catalyzed by intact bc_1 complex may result from (1) the limited accessibility of molecular oxygen to the Q_P pocket which is surrounded by structured protein subunits; (2) molecular oxygen competing unfavorably with heme b_L for the electron during bifurcated ubiquinol oxidation and thus few electrons are readily available for oxygen to react with; and (3) the $O_2\cdot^-$ being generated within the Q_P pocket may not easily escape to the aqueous medium.

Although intact protein subunits of the complex are not directly involved in superoxide generation, they form a barrier for the Q_P pocket to limit accessibility of molecular oxygen to the pocket. Destruction of protein structural integrity by heme deletion, heat inactivation, or proteiase K digestion leads to a loosening of the structural integrity of the Q_P pocket to facilitate the molecular oxygen to get access to the Q_P pocket and to ease the release of produced $O_2^{\cdot-}$ to the aqueous medium.

In this proposed mechanism, we speculate that the electron transfer between cytochrome *c* and QH_2 takes place at the surface of the lipid bilayer and that between QH_2 and O_2 occurs concurrently inside the lipid bilayer. This speculation is supported by the observations that reduction of cytochrome *c* by QH_2 is much slower under anaerobic conditions than that in the presence of oxygen; and the higher oxygen solubility in the hydrophobic environment than in the aqueous medium. In addition, it is also possible that an oxygen molecule is located between the 4-HO- group of QH_2 and heme b_L to mediate electron transfer between them in the hydrophobic environment of the Q_P pocket. If this were the case, one would expect to see a higher presteady state reduction rate of cytochrome *b* by ubiquinol in the presence of oxygen than in the absence of it. Our

preliminary results seem to support this speculation. Further investigation on the role of oxygen in the reduction of cytochrome *b* by ubiquinol is currently in progress in our laboratory.

Summary

When bc_1 is incubated at 37 ˚C, or digested with proteinase K at room temperature, the electron transfer activity decreases, whereas superoxide generating activity increases with increasing digestion time. Maximum superoxide production is obtained when the protein components of the complex are digested or denatured, at which point all the electron transfer activity is lost. This result indicates that superoxide generation by bc_1 does not require the presence of intact protein subunits. This, together with the observation that superoxide is produced upon oxidation of ubiquinol by a high potential oxidant, such as cytochrome *c* or ferricyanide, in the presence of phospholipid vesicles or micellar solution of detergents, encouraged us to propose that superoxide production takes place at the hydrophobic environment of the Q_P pocket through bifurcated oxidation of ubiquinol by transferring two electrons to a high potential electron acceptor ISC and to another electron acceptor molecular oxygen. The structural integrity of the protein subunits regulates the accessibility of molecular oxygen to and releasing of produced superoxide from the Q_P pocket and does not directly participate in superoxide production.

References

1. Loschen, G., Azzi, A., and Floh, L. (1973) *FEBS Letters* **33**, 84-88.
2. Loschen, G., Azzi, A., Richter, C., and Floh, L. (1974) *FEBS Letters* **42**, 68-72.
3. Boveris, A., and Chance, B. (1973) *Biochem. J.* **134**, 707-716.
4. McCord, J. M., and Fridovich, I. (1969) *J. Biol. Chem.* **244**, 6049-6055.
5. Boveris, A., Oshino, N., and Chance, B. (1972) *Biochem. J.* **128**, 617-630.
6. Korshunov, S. S., Skulachev, V. P., and Starkov, A. A. (1997) *FEBS Lett*. **416**, 15-18.
7. Galkin, A., and Brandt, U. (2005) *J. Biol. Chem.* **280**, 30129-30135.
8. Ohnishi, S. T., Ohnishi, T., Muranaka, S., Fujita, H., Kimura, H., Uemura, K., Yoshida, K.-i., and Utsumi, K. (2005) *Journal of Bioenergetics and Biomembranes* **37**, 1-15.
9. Genova, M. L., Ventura, B., Giuliano, G., Bovina, C., Formiggini, G., Parenti Castelli, G., and Lenaz, G. (2001) *FEBS Letters* **505**, 364-368
10. Muller, F. L., Liu, Y., Abdul-Ghani, M. A., Lustgarten, M. S., Bhattacharya, A., Jang, Y. C., and Van Remmen, H. (2008) *Biochem. J.* 409, 491–499.
11. Turrens, J. F., Alexandre, A., and Lehninger, A. L. (1985) *Arch. Biochem. Biophys* **237**, 408-414.
12. Nohl, H., and Jordan, W. (1986) *Biochem. Bioph. Res. Co.* **138**, 533-539.
13. Zhang, L., Yu, L., and Yu, C.-A. (1998) *J. Biol. Chem.* **273**, 33972-33976.
14. Muller, F., Crofts, A. R., and Kramer, D. M. (2002) *biochemistry* **41**, 7866-7874.
15. Sun, J., and Trumpower, B. L. (2003) *Arch. Biochem. Biophys.* **419**, 198-206.
16. Rottenberg, H. , Covian, R. and Trumpower, B. L. (2009) *J. Biol. Chem.* 284, 19203-19210.

17. Forquer, I., Covian, R., Bowman, M. K., Trumpower, B. L., and Kramer, D. M. (2006) *J. Biol. Chem.* **281**, 38459-38465.

18. Yu, C. A., and Yu, L. (1982) *Biochemistry* **21**, 4096-4101.

19. Tian, H., Yu, L., Mather, M. W., and Yu, C.-A. (1998) *J. Biol. Chem.* **273**, 27953-27959.

20. Yang, S.-Q., Ma, H.-W., Yu, L. and Yu, C.-A. (2008) *J. Biol. Chem.* ***283***, 28767-28776.

21. Tso, S-C., Yin, Y., Yu, C-A. and Yu, L. (2006) *Biochim. Biophys. Acta.* **1757**, 1561-1567.

22. Yu, C.-A., and Yu, L. (1980) *Biochim. Biophys. Acta* **591**, 409-420.

23. Yu, L., Yang, S-Q., Yin, Y., Cen, X-W., Zhou, F., Xia, D. and Yu, C-A. (2009) *Methods Enzymol.* **456**, 459-473.

24. Kagawa, Y., and Racker, E. (1971) *J. Biol. Chem.* **246**, 5477-5487.

25. Nakano, M. (1990) *Methods Enzymol.* **186**, 585-591.

26. Denicola, A., Souza, J., Gatti, R. M., Augusto, O., and Radi, R. (1995) *Free Radical Bio. Med.* **19**, 11-19.

27. Helenius, A., McCaslin, D.R., Fries, E. and Tanford, C. (1979) *Methods Enzymol.* **56**, 734-749.

VITA

YING YIN

Candidate for the Degree of

Doctor of Philosophy

Thesis: THE ROLE OF PROTEIN SUBUNITS IN SUPEROXIDE GENERATION BY THE CYTOCHROME bc_1 COMPLEX FROM *RHODOBACTER SPHAEROIDES*

Major Field: Biochemistry and Molecular Biology

Biographical:

Education: Received Bachelor of Science degree in Biology from Sichuan University, Chengdu, Sichuan, China in June 2003; Completed the requirements for the Doctor of Philosophy degree with a major in Biochemistry and Molecular Biology at Oklahoma State University in Dec. 2009.

Professional Memberships:
American Biophysical Society;
Biochemistry and Molecular Biology Graduate Student Association at Oklahoma State University.

Publications:

Tso, S. C., **Yin, Y**., Yu, C. A., Yu, L. (2006) *Biochim. Biophys. Acta.* **1757**,1561-1567;
Yu, C. A., Cen, X.W., Ma, H.W., **Yin, Y.**, Yu, L., Esser, L., and Xia, D. *Biochim. Biophys. Acta.* **1777**(7-8):1038-43;
Yu, L., Yang, S., **Yin, Y.**, Cen, X., Zhou, F., Xia, D., Yu, C-A. *Methods Enzymol.* **456**: 459-73.
Yin, Y., Tso, S. C., Yu, C. A., Yu, L. (2009) *Biochim. Biophys. Acta.* **1787**,913-919;

Name: YING YIN Date of Degree: December, 2009
Institution: Oklahoma State University Location: Stillwater, Oklahoma

Title of Study: THE ROLE OF PROTEIN SUBUNITS IN SUPEROXIDE GENERATION BY THE CYTOCHROME bc_1 COMPLEX FROM *RHODOBACTER SPHAEROIDES*

Pages in Study: 106 Candidate for the Degree of Doctor of Philosophy
Major Field: Biochemistry and Molecular Biology

Scope and Method of Study:

The electron transfer activity of three-subunit core cytochrome bc_1 complex from *Rhodobacter sphaeroides* has only one fourth that of the wild type enzyme. The addition of subunit IV to the core complex restores the activity to the same level as that of wild type. Why does the lack of subunit IV make such difference ? What is the essential residue of subunit IV for the reconstitutive activity? What is the role of subunit IV during bc_1 catalysis. The proteinase K treated complex has the maximum superoxide production. What produces superoxide anion after the digestion? To answer these questions, we constructed various mutants of subunit IV, and in vitro reconstitute them to the core complex , meanwhile bc_1 activity assay, SDS-PAGE, DSC, and in vitro binding assay were used. We also measured the pre-steady state reduction rate of cytochrome *b* and c_1, as well as the superoxide generation by bc_1 complex and different oxidant in the presence of phospholipids vesicles or detergents..

Findings and Conclusions:

Our results suggested that a region of subunit IV containing residues 77-85 is essential for the interaction with the core complex to restore the bc_1 activity. Residues 81-84 are required for reconstitutive activity of subunit IV. The core complex produces four times as much superoxide anion as does the wild-type enzyme. The subunit IV decreases the electron leakage from the Q_P pocket during bc_1 catalysis. The oxidation of ubiquinol by a high potential oxidant such as cytochrome c and ferricyanide in the presence of phospholipid vesicles or micellar solution of detergent results in the generation of superoxide. This suggested that superoxide generation from oxidation of ubiquinol only requires a high potential oxidant and hydrophobic environment.

ADVISER'S APPROVAL: Dr. Chang-An Yu